Phytomedicine 128 (2024) 155493

Contents lists available at ScienceDirect

Phytomedicine

journal homepage: www.elsevier.com/locate/phymed

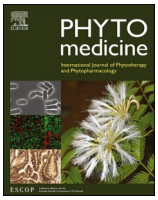

Original Article

Silibinin is a suppressor of the metastasis-promoting transcription factor ID3

Sara Verdura [a,b], José Antonio Encinar [c], Alexei Gratchev [d], Àngela Llop-Hernández [a,b], Júlia López [a,b], Eila Serrano-Hervás [a,b], Eduard Teixidor [e,f], Eugeni López-Bonet [b,g], Begoña Martin-Castillo [b,h], Vicente Micol [c,i], Joaquim Bosch-Barrera [e,f,j,1], Elisabet Cuyàs [a,b,1], Javier A. Menendez [a,b,1,*]

[a] *Program Against Cancer Therapeutic Resistance (ProCURE), Catalan Institute of Oncology, Girona, 17007, Spain*
[b] *Metabolism and Cancer Group, Girona Biomedical Research Institute (IDIBGI), Girona 17190, Spain*
[c] *Institute of Research, Development and Innovation in Health Biotechnology of Elche (IDiBE), Universitas Miguel Hernández (UMH), Elche 03202, Spain*
[d] *Laboratory for Tumor Stromal Cell Biology, Institute of Carcinogenesis, Nikolaj Nikolajevich (N.N.) Blokhin National Medical Research Center of Oncology, Moscow 115478, Russia*
[e] *Precision Oncology Group (OncoGir-Pro), Girona Biomedical Research Institute (IDIBGI), Girona 17190, Spain*
[f] *Medical Oncology, Catalan Institute of Oncology, Girona, 17007, Spain*
[g] *Department of Anatomical Pathology, Dr. Josep Trueta Hospital of Girona, Girona 17007, Spain*
[h] *Unit of Clinical Research, Catalan Institute of Oncology, Girona, 17007, Spain*
[i] *CIBER Fisiopatología de la Obesidad y la Nutrición (CIBEROBN), Instituto de Salud Carlos III (ISCIII), Madrid, 28029, Spain*
[j] *Department of Medical Sciences, Medical School, University of Girona, Girona, Spain*

ARTICLE INFO

Keywords:
Lung cancer
ID3
Milk thistle
Silibinin
Bone morphogenic proteins
SMAD

ABSTRACT

Background: ID3 (inhibitor of DNA binding/differentiation-3) is a transcription factor that enables metastasis by promoting stem cell-like properties in endothelial and tumor cells. The milk thistle flavonolignan silibinin is a phytochemical with anti-metastatic potential through largely unknown mechanisms.
Hypothesis/purpose: We have mechanistically investigated the ability of silibinin to inhibit the aberrant activation of ID3 in brain endothelium and non-small cell lung cancer (NSCLC) models.
Methods: Bioinformatic analyses were performed to investigate the co-expression correlation between *ID3* and bone morphogenic protein (BMP) ligands/BMP receptors (BMPRs) genes in NSCLC patient datasets. ID3 expression was assessed by immunoblotting and qRT-PCR. Luciferase reporter assays were used to evaluate the gene sequences targeted by silibinin to regulate *ID3* transcription. *In silico* computational modeling and LanthaScreen TR-FRET kinase assays were used to characterize and validate the BMPR inhibitory activity of silibinin. Tumor tissues from NSCLC xenograft models treated with oral silibinin were used to evaluate the in vivo anti-ID3 effects of silibinin.
Results: Analysis of lung cancer patient datasets revealed a top-ranked positive association of *ID3* with the BMP9 endothelial receptor ACVRL1/ALK1 and the BMP ligand BMP6. Silibinin treatment blocked the BMP9-induced activation of the ALK1-phospho-SMAD1/5-ID3 axis in brain endothelial cells. Constitutive, acquired, and adaptive expression of ID3 in NSCLC cells were all significantly downregulated in response to silibinin. Silibinin blocked ID3 transcription via BMP-responsive elements in *ID3* gene enhancers. Silibinin inhibited the kinase activities of BMPRs in the micromolar range, with the lower IC_{50} values occurring against ACVRL1/ALK1 and

Abbreviations: bHLH, basic helix-loop-helix; BBB, blood-brain barrier (BBB); BMP, bone morphogenic protein; BMPR, bone morphogenic protein receptor; BRE, BMP-responsive element; CSC, Cancer Stem Cell; DMSO, Dimethyl sulfoxide; ECS, Endothelial cells; FBS, Fetal bovine serum; HRP, horseradish peroxidase; IPSCS, induced pluripotent stem cells; ID, Inhibitor of DNA binding/differentiation; LUAD, lung adenocarcinoma; MEC, Microvascular endothelial cell; NSCLC, non-small cell lung cancer; PBS, phosphate buffered saline; QRT-QPCR, quantitative real-time polymerase chain reaction; SDS-PAGE, sodium dodecyl sulfate polyacrylamide gel electrophoresis; SMAD, Mothers against decantaplegic homolog; TBST, Tris-buffered saline containing Tween.

* Corresponding author.
E-mail address: jmenendez@idibgi.org (J.A. Menendez).
[1] J.A.M, E.C., and J. B-B. share senior authorship

https://doi.org/10.1016/j.phymed.2024.155493
Received 21 November 2023; Received in revised form 31 January 2024; Accepted 26 February 2024
Available online 6 March 2024

BMPR2. In an in vivo NSCLC xenograft model, tumoral overexpression of ID3 was completely suppressed by systematically achievable oral doses of silibinin.
Conclusions: ID3 is a largely undruggable metastasis-promoting transcription factor. Silibinin is a novel suppressor of ID3 that may be explored as a novel therapeutic approach to interfere with the metastatic dissemination capacity of NSCLC.

Introduction

The inhibitor of DNA-binding/differentiation (ID) proteins ID1–4 are transcriptional regulators that control cell differentiation by interfering with the DNA-binding activity of basic helix-loop-helix (bHLH) transcription factors (Lasorella et al., 2014; Perk et al., 2005; Roschger and Cabrele, 2017). ID proteins transcriptionally synchronize the determination of cell fate with the appropriate extracellular interactions in the niche microenvironment, thereby inhibiting differentiation and maintaining the self-renewal and multipotency capacity of stem/progenitor cells during development (Niola et al., 2012). ID protein expression is largely silent in most adult tissues, but can be reactivated in various disease processes such diabetes, Diamond-Blackfan anemia, Rett syndrome, and cancer (Ling et al., 2014; Wang and Baker, 2015). ID proteins are highly expressed in virtually all human tumors, where their presence in the cancer cell compartment and/or in the tumor vasculature is associated with an aggressive phenotype and a poor clinical outcome (Anido et al., 2010; Castañon et al., 2013; Lee et al., 2004; Lyden et al., 1999; Maw et al., 2008; Ponz-Sarvisé et al., 2011; Schindl et al., 2003; Schoppmann et al., 2003; Sharma et al., 2012). *ID* gene expression confers tumor-initiating capacity and chemo-/-radio-resistance to certain subpopulations of cancer stem cell (CSC)-like cells in the context of primary tumorigenesis and during the early stages of metastatic colonization (Gupta et al., 2007; Iavarone and Lasorella, 2006; Ke et al., 2018; Stankic et al., 2013). ID proteins can exert extrinsic actions to promote metastatic dissemination by remodeling the tumor microenvironment and promoting the activation and recruitment of endothelial cells (ECs) to support tumor angiogenesis at the primary and metastatic sites (Benezra, 2011; Gao et al., 2008). Activation of IDs further contributes to the stemness of ECs, a phenomenon that may facilitate not only the passage of brain metastatic cells across the blood-brain barrier (BBB), but also the reorganization of the cerebral microvasculature in reactive niches of primary and secondary brain tumors (Das and Felty, 2014,2015; Das et al., 2015, 2022; Perez et al., 2023; Perez and Felty, 2022).

Disrupting the ID-driven cancer cell-intrinsic and extrinsic regulatory actions may provide additive or even synergistic anti-metastastic effects. However, transcription factors such as ID proteins are notoriously difficult to target with small molecule inhibitors (Nair et al., 2014; Wojnarowicz et al., 2021). First, with the exception of Burkitt's lymphoma (Richter et al., 2012), mutations or genomic rearrangements in the *ID* genes or their promoters are rarely found in most human malignancies. Second, although the feasibility and anti-tumor effects of systemic ID protein targeting have been supported by using siRNA/anti-sense oligonucleotides delivery systems and cell permeable peptides that target ID proteins for degradation (Mern et al., 2010), the effectiveness of directly inactivating ID proteins might depend on the largely unknown biochemical nature of the ID proteins-containing transcriptional complexes. Third, although a valuable alternative is to target *ID* gene expression rather than ID function, one should acknowledge that cancer-associated reactivation of IDs is due to the convergence of numerous and diverse signaling cascades (e.g., MAPK kinase, Myc, Src, FLT3, VEGF, Wnt, Notch) on the *ID* gene promoters (Nair et al., 2014). Although a small molecule pan-ID antagonist (AGX51) has been shown to phenocopy the effects of *ID1* and *ID3* gene loss to regress therapy-resistant tumor growth and suppress metastatic colonization (Wojnarowicz et al., 2019, 2021), targeted pharmacologic inhibition of ID3 has been unavailable, even in preclinical cancer models. The bone morphogenic protein (BMP) signaling pathway, the major upstream regulator of ID expression in cell biology, may provide an alternate therapeutic path to target ID proteins including ID3. BMPs mediate cancer cell fate decisions, including proliferation, survival, and self-renewal cues, through transcriptional regulation of ID1/3 (Hayashi et al., 2016; Hollnagel et al., 1999; Kowanetz et al., 2004; Ying et al., 2003). Inhibition of BMP signaling decreases cell growth, induces cell death, and reduces stemness of cancer cells by down-regulating ID1/3 proteins. Several generations of small-molecule ATP-competitive inhibitors with varying affinity for the kinase domain of BMP type I and type II receptors (BMPR), such as dorsomorphin, LDN-193,189, DMH-2, and JL-5, have been shown to act predominantly as ID1 (but not ID3) inhibitors (Langenfeld et al., 2013a).

The flavonolignan silibinin, the major bioactive component of silymarin extract from *Silybum marianum* (milk thistle) seeds, is a phytochemical with a well-established chemopreventive capacity to suppress tumor initiation and progression, but also with therapeutic potential to target metastatic progression (Bosch-Barrera and Menendez, 2015; Bosch-Barrera et al., 2017, 2021; Deep and Agarwal, 2010; Mateen et al., 2013). Pre-clinical studies have repeatedly demonstrated the ability of silibinin to suppress signaling pathways involved in metastasis-related phenomena including adhesion, motility, invasiveness, and epithelial-to-mesenchymal transition (EMT) (Cufí et al., 2013a; Verdura et al., 2021, 2022) by targeting not only not only cancer cells but also supporting components of the tumor microenvironment such as ECs (Deep and Agarwal, 2013; Deep et al., 2017; Mirzaaghaei et al., 2019). Therapeutic interventions with a silibinin-based nutraceutical (Legasil®) have demonstrated the groundbreaking activity of silibinin against established brain metastases (BM), but not against extracranial disease progression, in heavily pretreated non-small cell lung cancer (NSCLC) patients (Bosch-Barrera et al., 2017; Priego et al., 2018). As previously demonstrated in models of ischemic stroke (Wang et al., 2012), the significant improvement in overall survival of silibinin-treated NSCLC patients was accompanied by a marked reduction or prevention of tumor-associated vasogenic edema in BM lesions (Bosch-Barrera et al., 2017; Priego et al., 2018). Vasogenic edema result from the breakdown of the blood-brain barrier (BBB) (Solar et al., 2022), which composed of interacting cells such as ECs, pericytes, and astrocytes, strongly indicating that the anti-BM activity of silibinin may involve a reprogramming of BM-associated non-tumoral cell types (Priego and Valiente 2019; Wasilewski et al., 2017).

Here, we investigated the mechanistic ability of silibinin to specifically target the expression of the largely undruggable metastasis-promoting *ID3* transcription factor in brain ECs and NSCLC cells. Combining experimental efforts with cultured ECs and NSCLC cell models, luciferase reporter assays with regulatory sequences of the *ID3* gene, *in silico* computational studies using docking and molecular dynamics simulations, and in vitro studies with purified BMPR kinases, we now present the first evidence that silibinin represses both the inducible expression of ID3 in the brain vasculature as well as the constitutive, acquired and adaptive expression of ID3 in therapy-resistant NSCLC cells.

Materials and methods

ID3 gene correlations in lung cancer patients

Gene-level expression files were downloaded from the cBioportal for

Cancer Genomics (https://www.cbioportal.org) for The Cancer Genome Atlas Lung Adenocarcinoma Collection (TCGA-LUAD) study, which includes RNAseq data from 510 samples. Patients/samples were categorized based on *z*-score ±1 threshold relative to all samples into high or low *ID3* mRNA expression groups. Person correlation analysis was performed in tumor samples between *ID3* and several genes encoding proteins involved in the BMP signaling pathway. These genes include BMP ligands, activin/inhibins, GDFs, and BMP receptors.

Cell lines and culture conditions

Human NSCLC cell lines A549 (ATCC CCL-185), H460 (ATCC HTB-177), H1993 (ATCC CRL-5909), and H1975 (ATCC CRL-5908), and HEK293T (ATCC CRL-3216) were obtained from the ATCC (Manassas, VA, USA). The Human Cerebral Microvascular Endothelial Cell (MEC) Line hCMEC/D3 (#CLU512-A) was obtained from Cedarlane Laboratories Limited/Tebu-Bio (Burlington, NC, USA). H3122 (CVCL_5160) and H2228 (ATCC CRL-5935) cell lines, harboring the E13:A20 and E6a/b:A20 variants of the EML4-ALK fusion, respectively, were rendered resistant to crizotinib (H3122/CR and H2228/CR) by incremental and continuous exposure to crizotinib, as previously described (Kim et al., 2013; Verdura et al., 2022; Yamaguchi et al., 2014). Parental PC-9 (RRID:CVCL_B260) cells harboring an EGFR activating mutation (Δ746–750) were obtained from the IBL Cell Bank (Gunma, Japan) and rendered resistant to erlotinib (PC-9/ER) by incremental and continuous exposure to erlotinib, as described (Vazquez-Martin et al., 2013).

A549, PC-9, PC-9/ER, and HEK293T cells were routinely expanded in Dulbecco's modified Eagle's medium (DMEM, Gibco) supplemented with 10 % heat-inactivated fetal bovine serum (FBS; Linus), 1 % l-glutamine, 1 % sodium pyruvate, 50 IU/ml penicillin, and 50 μg/ml streptomycin. H460, H1993, H1975, H3122, H3122/CR, H2228, H2228/CR were routinely expanded in RPMI 1640 (Gibco) supplemented with 10 % heat-inactivated FBS, 1 % l-glutamine, 50 IU/ml penicillin, and 50 μg/ml streptomycin. hCMEC/D3 cells were grown in EGM™−2 MV MEC Growth Medium-2 BulletKit™ containing EBM™-2 Basal Medium and EGM™-2 MV MEC Growth Medium SingleQuots™ supplements (#H3CC-3202) required for growth of MECs (Lonza) at the following concentrations: 0.025 % (*v/v*) rhEGF, 0.025 % (*v/v*) VEGF, 0.025 % (*v/v*) IGF, 0.1 % (*v/v*) rhFGF, 0.1 % (*v/v*) gentamicin, 0.1 % (*v/v*) ascorbic acid, 0.04 % (*v/v*) hydrocortisone, and 2.5 % (*v/v*) FBS as specified by Weksler et al. (2005). hCMEC/D3 cells were seeded onto tissue culture flasks were precoated with 1/100 collagen type I solution.

All cells were grown at 37 °C in a humidified atmosphere with 5 % CO_2 and were in the logarithmic growth phase at the beginning of the experiments. Cell lines were authenticated by STR profiling, both performed by the manufacturer and confirmed in-house at the time of purchase according to ATCC guidelines. Cells were passaged by starting a low-passage cell stock every month until to 2–3 months after resuscitation. Cell lines were screened for mycoplasma contamination using a PCR-based method for *Mycoplasma* detection prior to experimentation and were intermittently tested thereafter.

Drugs, reagents, and antibodies

Silibinin (Cat. #S0417; ≥ 98 % purity, HPLC area%) was purchased from Sigma-Aldrich (Madrid, Spain). BMP4 (Cat. #120–05), BMP6 (Cat. #120–06), TGFβ1 (Cat. #AF-100–21C-B), and GDF2 (BMP9; Cat. #120–07–1MG) human recombinant proteins were purchased from PeproTech® EC, Ltd (London, UK). Rabbit monoclonal antibody against ID3 (Cat. #BCH-4/#3–3) and ID1 (Cat. #BCH-1/#195–14) were purchased from BioCheck, Inc. (San Francisco, CA, USA). Rabbit polyclonal antibodies against SMAD2/3 (Cat. #3102), phospho-SMAD2 (Ser465/467)/SMAD3 (Ser423/425) (Cat. #9510), SMAD1 (Cat. #D59D7), SMAD5 (Cat. #D4G2), and SMAD1/5 (Ser463/465) (Cat. #41D10) were purchased from Cell Signaling Technology (Danvers, MA, USA). Mouse monoclonal antibodies against GAPDH (Cat. #60,004–1-Ig) and β-actin (Cat. #66,009–1-Ig) were purchased from Proteintech (Rosemont, IL, USA). Dorsomorphin (Cat. #S7840) and K02288 (Cat. #S7359) were purchased from Selleckchem (Houston, TX, USA). The Dual-Glo Luciferase Assay System (Cat. #E2920) and the FuGENE® Transfection Reagent (Cat. #E2691) were purchased from Promega Corporation (Madison, WI, USA).

MTT-Based cell viability assays

The concentration range of cytostatic versus cytotoxic effects of silibinin was assessed by MTT-based cell viability assays involving 72 h exposure to graded concentrations of silibinin as described elsewhere (Bosch-Barrera et al., 2021). The sensitivity of cell lines to silibinin was expressed as the concentration required to reduce cell viability by 50 % (IC_{50}; **Table S1**). Since the percentage of control absorbance was considered to be the surviving fraction of cells, the IC_{50} value was defined as the silibinin concentration that produced a 50 % reduction in control absorbance and was estimated using non-linear regression analyses of dose-response curves.

Luciferase assays

Functional identification and cloning of the *ID3* gene enhancers (ECR1 and ECR2) and *ID3* promoter regulatory sequences (BMP response element [BRE], CAGA boxes, bipartite BRE-CAGA enhancer elements) in ID3 reporter plasmids has been reported previously (Nurgazieva et al., 2015; Shepherd et al., 2008). HEK293T cells were transfected with ID3 reporter plasmids using the FuGENE® Transfection Reagent according to the manufacturer's instructions. Briefly, cells were seeded 1 day prior to transfection at a density of 5×10^5 cells per well in 6-well plates. For all reporter gene assays, 4 μg of the luciferase reporter plasmid was co-transfected with 40 ng of the *Renilla* reporter plasmid. Twenty-four hours after transfection, the cells were harvested and re-plated in a white 96-well plate that had been pre-coated with 0.1 % gelatin. The next day, the cells were stimulated with TGFβ, BMP4, BMP6 or BMP9 (all of them at 10 ng/ml) in the absence or presence of silibinin (100 μM/l), dorsomorphin (5 μM/l) or K02288 (1 μM/l) in medium containing 2 % FBS or left untreated, as indicated. All conditions were performed in duplicate. After 24 h of treatment, luciferase and *Renilla* activities were measured using the Dual-Glo Luciferase Assay System according to the manufacturer's instructions. Luminescence measurements were performed using a Cytation 5 plate reader (Biotek). The luciferase activity was first normalized to the Renilla activity and then referenced to the backbone of the corresponding empty plasmid.

Immunoblotting

Cells were seeded in 6-well plates at 200,000 – 250,000 cells/well and allowed to grow overnight in maintenance cell culture media containing 10 % FBS. Following overnight serum starvation, cells were cultured in the absence or presence of varied concentrations of silibinin in the corresponding media containing 2 % FBS (24 – 48 h). Cells were then washed with ice-cold phosphate buffered saline (PBS), and scraped immediately after adding 30 – 75 μl of 2 % SDS, 1 % glycerol, and 5 mM/l Tris–HCl, pH 6.8. The protein lysates were collected in 1.5 ml microcentrifuge tubes and samples were sonicated for 1 min (under ice water bath conditions) with 2 s sonication at 2 s intervals to fully lyse cells and reduce viscosity. Protein content was determined by the Bradford protein assay (Bio-Rad, Hercules, CA). Sample buffer was added and extracts were boiled for 4 min at 100 °C. Equal amounts of protein were electrophoresed on SDS-PAGE gels, transferred to nitrocellulose membranes and incubated with primary antibodies, followed by incubation with a horseradish peroxidase-conjugated secondary antibody and chemiluminescence detection. β-actin and GAPDH were employed as controls for protein loading. Densitometric values of protein bands were quantified using densitometry (Image J software, which can be readily

downloaded from the NIH website https://imagej.nih.gov/ij/download.html). All the protein bands used as loading controls (e.g., β-actin, GAPDH) were from the same blot as the proteins tested (uncropped/unedited Western blot images of the bands shown in the main figures are included in Supplementary **Fig. S1**).

Quantitative real-time polymerase chain reaction (qRT-PCR)

Total RNA was extracted from cells using the RNA Plus Kit (Macherey-Nagel, Germany) to the manufacturer's instructions. Two micrograms of total RNA was reverse-transcribed to cDNA using the High-Capacity cDNA Reverse Transcription Kit (Applied Biosystems, Waltham, MA). The abundance of *ID3* (Hs00171409_m1) was evaluated in technical replicates relative to the housekeeping genes *ACTB* (Hs99999903_m1) and *GAPDH* (Hs99999905_m1) using an Applied Biosystems QuantStudio™ 7 PCR System with an automated baseline and threshold cycle detection. The transcript abundance was calculated using the comparative C_t method and presented as relative quantification (RQ) or fold-change, as specified.

Docking calculations, molecular dynamics (MD) simulations, and binding free energy analysis

Docking calculation, MD simulations, molecular docking score ΔG (Gibbs free binding energy), binding affinity (Kd), and molecular mechanics Poisson–Boltzmann surface area (MM/PBSA) calculations to *in silico* assess the binding modes and the alchemical binding free energy of silibinin A and B against the 3D crystal structures 3MY0 (ACVRL1/ALK1), 3G2F (BMPR2), 3MDY (BMPR1B/ALK6), 4BGG (ACVR1/ALK2), 2QLU (ACVR2B/ActRIIB), and 3SOC (ACVR2A/ActRIIA) were performed using procedures described in previous works from our group (Cuyàs et al., 2019; Encinar and Menendez, 2020; Verdura et al., 2022). All of the figures were prepared using PyMol 2.0 software and all interactions were detected using the protein-ligand interaction profiler (PLIP) algorithm.

LanthaScreen kinase assays

To obtain 10-point titration results of the regulatory activity of silibinin on the ATP-dependent kinase activity of ACVRL1/ALK1, ACVR1/ALK2, BMPR1A/ALK3, BMPR2, BMPR1B/ALK6, ACVR2A/ActRIIA, ACVR2B/ActRIIB, LanthaScreen Eu kinase binding assays were outsourced to ThermoFisher Scientific using the SelectScreen™ Biochemical Kinase Profiling Service.

Animal studies

The effects of silibinin on ID3 protein expression *in vivo* were evaluated in archived, fresh frozen processed tumor tissues from erlotinib-refractory EGFR-mutant NSCLC mouse xenografts that were randomly assigned to receive by oral gavage vehicle control, erlotinib (100mg/kg, 5 days a week), silibinin-meglumine (100mg/kg, 5 days a week), or erlotinib *plus* silibinin-meglumine. Tumor cell implantation experiments in non-obese diabetic/severe combined immunodeficient (NOD/ SCID) mice were performed as described elsewhere (Cufí et al., 2013a,b) and approved by the Institutional Animal Care and Use Committee (IACUC) of the Institut d'Investigació Biomèdica de Bellvitge (IDIBELL; Animal Use Protocol #6302 approved by the Animal Experimental Commission of the Government of Catalonia, Barcelona, Spain; 11/17/2011). Tumor tissues were crushed into smaller pieces in dry ice to maintain the frozen state, lysed, and then subjected to SDS-PAGE as described above.

Statistical analysis

All cell-based observations were confirmed by at least three independent experiments performed in triplicate for each cell line and for each condition. Data are presented as mean ± SD. Bar graphs, curves, and statistical analyses were generated using GraphPad Prism 10 (GraphPad Software, San Diego, CA). Two-group comparisons were performed using Student's t-test for paired and unpaired values. Comparisons of means of ≥3 groups were performed by ANOVA, and the existence of individual differences, in the case of significant F values in ANOVA, was tested by Tukey's multiple contrasts. p values < 0.05 and <0.005 were considered to be statistically significant (denoted as * and **, respectively). All statistical tests were two-tailed.

Results

ID3 expression is associated with the BMP receptor ALK1/ACVRL1 and the BMP ligands BMP6/BMP2 in lung adenocarcinoma patients

Activation of *ID3* gene transcription is a highly complex output that is encoded in the various possible arrangements of specific BMP ligands and BMP receptor combinations that determine the signaling output of the BMP-SMAD signaling axis (Alsamarah et al., 2015; Antebi et al., 2017; Klumpe et al., 2022). Therefore, we evaluated the potential correlation between *ID3* expression levels and the expression of various BMP ligands and receptors in lung adenocarcinoma (LUAD), the most common histologic subtype of NSCLC. Using LUAD patient data available in the TCGA-LUAD database ($n = 510$), we evaluated and ranked the magnitude and *p*-value of the correlation between *ID3* expression and BMP ligands, activins/inhibins, GDFs, and BMP receptors (Fig. 1a).

Among the BMP receptors, the expression of *ACVRL1/ALK1* had the highest positive and statistically significant association with *ID3* ($r = 0.35$, $p < 0.0001$; Fig. 1a, *left panels*). When patients were stratified based on median *ID3* expression, patients with high *ID3* expression had significantly higher expression levels of the gene encoding for the type I BMP receptor *ACVRL1/ALK1* (Fig. 1B, top *panels*). Endoglin (*ENG*), a co-receptor for the high-affinity ligand for ALK1 BMP9, was also significantly associated with the expression of *ID3* in LUAD patients ($r = 0.27$, $p < 0.0001$). Among the ligands, *BMP6* expression showed the highest positive and statistically significant association with *ID3* ($r = 0.38$, $p < 0.0001$; Fig. 1A, *right panels*). When patients were stratified based on median *ID3* expression, patients with high *ID3* expression had significantly higher levels of *BMP6* (Fig. 1b, *bottom panels*). This suggests that high levels of the BMP ligand BMP6 may act as a potential driver of ID3 in LUAD. *BMP2* was also significantly associated with the expression of *ID3* in LUAD patients ($r = 0.35$, $p < 0.0001$).

Silibinin inhibits the BMP9-ALK1-SMAD1/5-ID3 signaling pathway in endothelial cells

Given that the endothelial cell-restricted *ACVRL1/ALK1* receptor (Alsina-Sanchís et al., 2018) was significantly associated with *ID3* expression in LUAD patients, we first explored if the presence of silibinin may modify the ability of the ALK1 ligand BMP9 to activate the ALK1-SMAD1/5-ID3 signaling pathway in ECs. To address this question, we selected a clinically-relevant human brain microvascular model of ECs namely the hCMEC/D3 cells (Weksler et al., 2005), which acquire an *ID3*-driven stem cell-like signature in response to microvascular injury and are widely used as a valuable model of human BBB permeability and brain metastatic cell crossing (Das and Felty, 2014, 2015; Das et al., 2015).

Immunoblotting confirmed that the addition of BMP9 strongly enhanced the SMAD1/5 phosphorylation and robustly upregulated the expression of ID3 protein in hCMEC/D3 ECs. Although TGFβ has been shown to induce lateral activation of SMAD1/5 via TβR1/ALK5 and ALK1 complexes in embryonic ECs (Hiepen et al., 2019, 2020), TGFβ treatment has no effect on either phospho-SMAD1/5 or ID3 status in hCMEC/D3 ECs (Fig. 2a). BMP9 can also phosphorylate SMAD2 through heterodimeric complexes of ALK1/ActR2 in HUVEC ECs (Hiepen et al., 2019, 2020), but we did not observe any activation of SMAD2 in

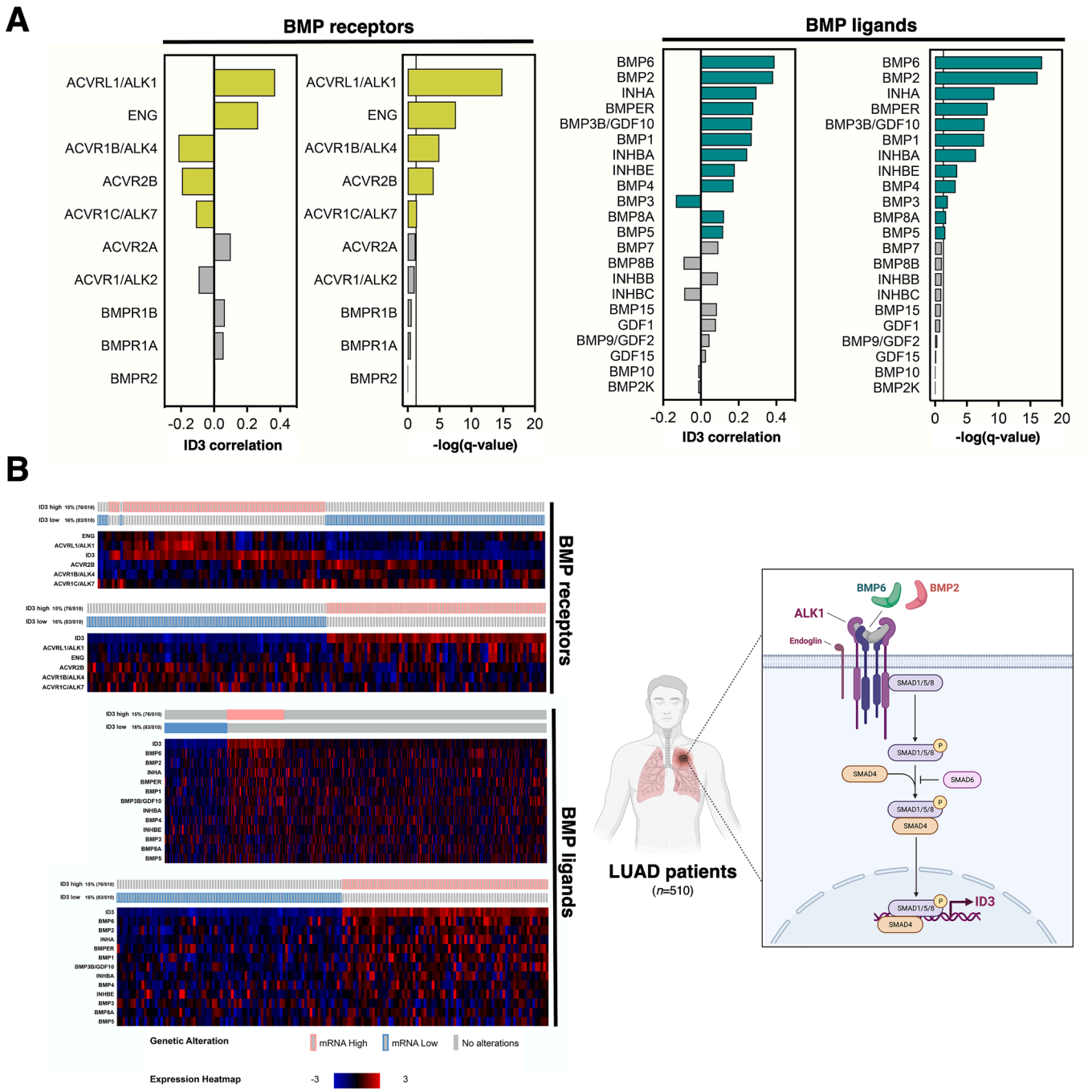

Fig. 1. Correlation of ID3 with the expression levels of BMP ligands and BMP receptors in patients with lung adenocarcinoma (LUAD). A. Pearson correlation coefficients and *p*-values between *ID3* mRNA expression levels and several BMP receptor (*left panels*) and BMP ligand (*right panels*) genes in patients with LUAD ($n = 510$). B. cBioPortal "oncoprint" representation of co-alterations in ID3 and BMP receptor genes (*left panels*) and BMP ligands (*right panels*). Numbers indicate the frequency of *ID3* mRNA expression changes (low/high). *Inset schematic: ID3* expression is positively correlated with the mRNA expression levels of specific members of the BMP/BMPR signaling pathway (i.e., ALK1/ENG receptors and BMP6/BMP2 ligands) in patients with LUAD.

response to either BMP9 or TGFβ in hCMEC/D3 ECs (Fig. 2a). Taken together, these results confirmed that hCMEC/D3 ECs are an ideal model to evaluate the ability of silibinin to inhibit the BMP9-ALK1-SMAD1/5-ID3 signaling pathway. Addition of silibinin significantly reduced BMP9-induced SMAD1/5 phosphorylation and completely blunted the downstream upregulation of ID3 protein in a time-dependent manner (Fig. 2b). Although with different temporal dynamics, silibinin was as efficient as the potent ALK1 inhibitor K02288 (Chen et al., 2021; Sanvitale et al., 2013) in preventing BMP9-stimulated activation of SMAD1/5 and ID3 protein expression. We then verified that the ability of silibinin to impede the BMP9 up-regulatory signaling on ID3 expression occurred at the transcriptional level by assessing the effect of silibinin and K02288 on BMP9-induced *ID3* gene expression in hCMEC/D3 ECs using quantitative real-time PCR (qRT-PCR). The drastic induction of *ID3* mRNA occurring upon stimulation with BMP9 was significantly prevented in the presence of silibinin, largely mimicking the inhibitory activity of the selective type I BMP receptor inhibitor K02288 (Fig. 2b).

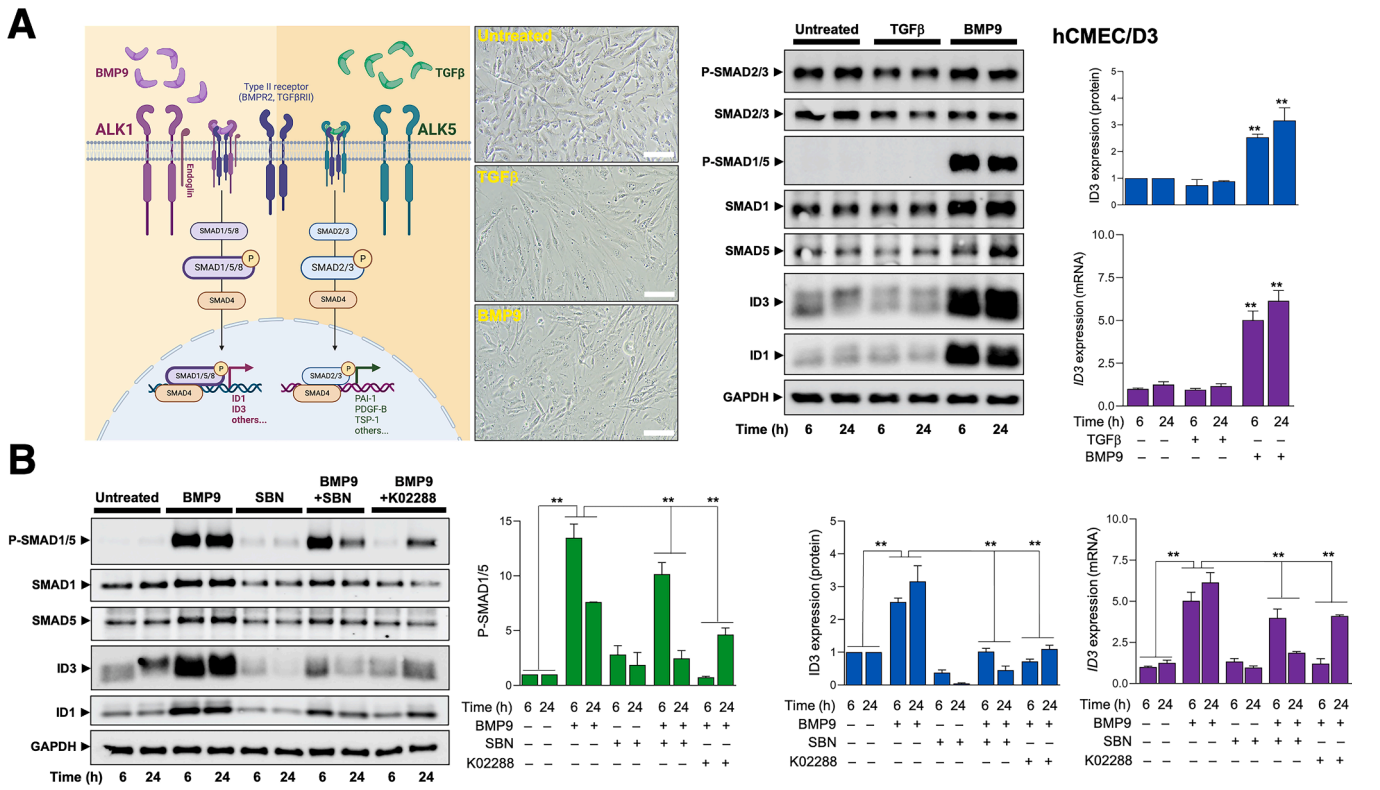

Fig. 2. Silibinin inhibits the BMP9-ALK1-SMAD1/5-ID signaling axis in cerebral endothelial cells. A. *Left panel.* BMP9 binds only ALK1, whereas TGFβ activates both ALK1 and ALK5 type I receptors expressed in ECs. In addition, endoglin acts as a co-receptor that modulates signaling through ALK1. SMAD 1 and 5 are preferentially phosphorylated and activated by ALK1, whereas SMAD 2 and 3 act as downstream effectors of ALK5. Subsequently, the SMADs are translocated to the nucleus, where they regulate the expression of specific genes (e.g., ID3/ID1 through phospho-SMAD1/5) (Cunha and Pietras, 2011). *Middle panels.* Representative brightfield microscopy images of hCMEC/D3 cells showing changes in cell morphology after BMP9 (10 ng/ml) and TGFβ (10 ng/ml) treatments for 3 days. Scale bar= 100 μm. *Right panels.* Expression levels of P-SMAD2/3, SMAD2/3, P-SMAD1/5, SMAD1, SMAD5, ID3, and ID1 proteins were detected by immunoblotting in lysates of hCMEC/D3 cells stimulated with TGFβ (10 ng/ml) or BMP9 (10 ng/ml) for 6 and 24 h using specific antibodies. The figures show representative immunoblots from multiple ($n \geq 3$) independent experiments. Intensity of ID3 protein bands was measured using the ImageJ software and the fold-change relative to untreated cells was calculated using GAPDH as a loading control. *ID3* transcript abundance was calculated using the $\Delta\Delta C_t$ method and presented as relative expression; ** $p < 0.005$, statistically significant differences relative to untreated cells. B. *Left panel.* Expression levels of P-SMAD1/5, SMAD1, SMAD5, ID3, and ID1 proteins were detected by immunoblotting in lysates from hCMEC/D3 cells stimulated with BMP9 (10 ng/ml) in the absence or presence of either silibinin or K02288. Figures show representative immunoblots of multiple ($n \geq 3$) independent experiments. *Right panels.* The intensity of the P-SMAD1/5 and ID3 protein bands was measured using the ImageJ software and the fold-change relative to untreated cells was calculated using GAPDH as a loading control. *ID3* transcript abundance was calculated using the $\Delta\Delta C_t$ method and presented as relative expression; *$p < 0.05$, ** $p < 0.005$, statistically significant differences.

Silibinin suppresses constitutive, acquired, and adaptive upregulation of ID3 expression in NSCLC cells

We then investigated the ability of silibinin to regulate ID3 protein expression in a broad panel of NSCLC cell lines with epithelial (E), mesenchymal (M) or mixed epithelial/mesenchymal (E/M) phenotypes (Schliekelman et al., 2015; Thomson et al., 2005; Verdura et al., 2022). Constitutive overexpression of the ID3 protein was detected exclusively in NSCLC models enriched with mesenchymal-like cell subpopulations, such as H460 and A549, the hybrid E/M cell line PC-9 and its erlotinib-resistant derivative PC-9/ER, which showed a further enrichment of EMT-related morphological and transcriptional features (Cuff et al., 2013a,b; Vazquez-Martin et al., 2013), but not in the epithelial-like H3122 and H1993 cells (*Fig. 3A, top panel*). Notably, ID3 overexpression was an acquired trait in H2228/CR cells, which are derived from ID3-low H2228 epithelial cells by stepwise selection with increasing concentrations of the ALK tyrosine kinase inhibitor (TKI) crizotinib over a period of 8 months and exhibit multiple EMT features driving cross-resistance to next-generation ALK TKIs (Kim et al., 2013; Verdura et al., 2022). In all ID3-positive NSCLC cell models tested, namely H460, A549, PC-9, PC-9/ER and H2228/CR, silibinin treatment significantly downregulated or completely suppressed ID3 protein overexpression in a dose- and time-dependent manner (Fig. 3b, *left panels*). The regulatory effects of silibinin on ID3 cannot be attributed to general (or basal) cytotoxicity based on the inhibitory concentrations ($IC_{20,50}$) calculated after 72 h of silibinin exposure by MTT assay (**Table S1**). qRT-PCR analysis confirmed that the levels of *ID3* mRNA were significantly up-regulated in the mesenchymal-like NSCLC cell models that over-expressed the ID3 protein, indicating that specific changes in *ID3* mRNA expression closely correspond to changes in ID3 protein expression status in NSCLC cells (Fig. 3a, *bottom panel*). To determine whether silibinin could downregulate *ID3* expression at the mRNA level in NSCLC cells as it did in ECs, we used H2228/CR cells as a model of acquired ID3 overexpression (up to 7-fold higher *ID3* mRNA compared to parental H2228 cells). Treatment with silibinin reduced the *ID3* transcript levels by a factor of several fold in a dose- and time-dependent manner, even below the baseline levels observed in the parental H2228 cells (Fig. 3b, *right panels*).

Exposure of parental H2228 cells to multi-generation ALK TKIs, including crizotinib, brigatinib, and lorlatinib, promoted significant phospho-activation of SMAD1/5 (Fig. 3c). This was accompanied by upregulation of ID3 at both protein and mRNA levels. Silibinin and the pan-type BMPR inhibitor dorsomorphin, but not K02288 (with increased selectivity for ALK1 and ALK2 over other type I BMP receptors and reduced off-targets compared to dorsomorphin), prevented ALK TKIs-induced upregulation of ID3 protein and *ID3* transcripts, while

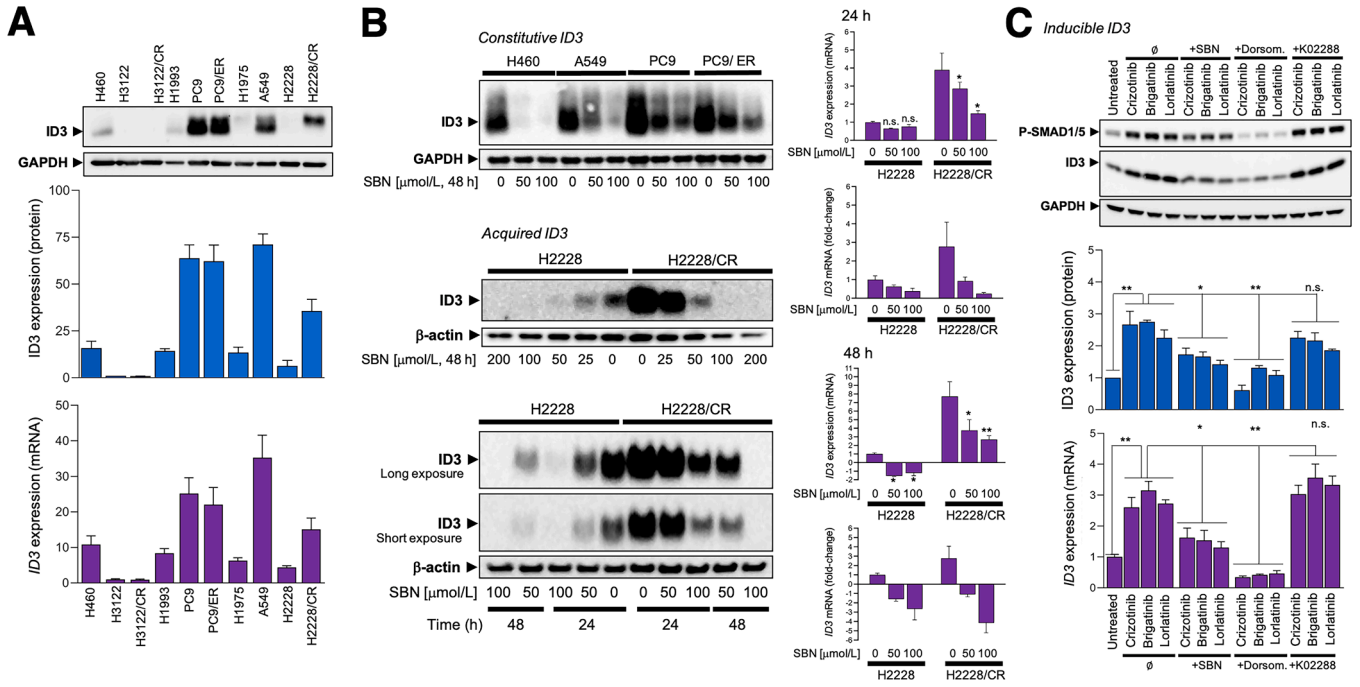

Fig. 3. Silibinin prevents constitutive, acquired, and inducible ID3 expression in NSCLC cells. A. *Top panel.* Basal expression levels of the ID3 protein were detected by immunoblotting in lysates from NSCLC cell lines using a specific anti-ID3 antibody. Shown is a representative immunoblot from multiple ($n \geq 3$) independent experiments. *Bottom panels.* The intensity of the ID3 protein bands was measured using the ImageJ software and the fold-change relative to untreated cells was calculated using GAPDH as a loading control. *ID3* transcript abundance was calculated using the $\Delta\Delta C_t$ method and presented as relative expression. B. *Left panels.* Expression levels of ID3 were detected by immunoblotting in NSCLC cell models grown in the absence/presence of graded concentrations of silibinin for 24 or 48 h. The intensity of the ID3 protein bands was measured using the ImageJ software. The fold change of each protein relative to untreated samples was calculated using GAPDH as a loading control. The figure shows representative immunoblots from multiple ($n \geq 3$) independent experiments. *Right panels. ID3* transcript abundance of was calculated using the $\Delta\Delta C_t$ method and presented as either relative or fold-change expression (compared to untreated H2228 parental cells) expression. *$p < 0.05$, ** $p < 0.005$, statistically significant differences. n.s. not significant. C. *Top panel.* Expression levels of P-SMAD1/5 and ID3 proteins were detected by immunoblotting in lysates from H2228 NSCLC cells exposed to the ALK-TKIs crizotinib, brigatinib, and lorlatinib (1 μM/l each) for 24 h in the absence or presence of either silibinin (100 μM/l) or K02288 (1 μM/l). Shown are representative immunoblots from multiple ($n \geq 3$) independent experiments. *Bottom panels.* The intensity of the P-SMAD1/5 and ID3 protein bands was measured using the ImageJ software and the fold-change relative to untreated cells was calculated using GAPDH as a loading control. *ID3* transcript abundance was calculated using the $\Delta\Delta C_t$ method and presented as relative expression; *$p < 0.05$, ** $p < 0.005$, statistically significant differences. n.s. not significant.

reducing ALK TKIs-induced phospho-activation of SMAD1/5 (Fig. 3c).

Silibinin transcriptionally suppresses ID3 gene expression via BMP-responsive elements

The above results suggest that silibinin could cause a decrease in *ID3* mRNA levels by inhibiting *ID3* gene transcription. To further confirm that silibinin can transcriptionally attenuate the BMP/SMAD1/5-mediated regulation of *ID3* gene expression, we used previously generated reporter plasmids with or without SMAD1/5-responsive enhancers or BMP-responsive elements in the regulatory sequences of the human *ID3* gene (Nurgazieva et al., 2015; Shepherd et al., 2008). Bioinformatics analysis of novel, potentially SMAD-dependent regulatory elements in the *ID3* gene has allowed the identification of enhancers located between −3177 and −2660 bp upstream of the transcription start site (i.e., a so-called evolutionary conserved region [ECR] 1) and ECR2 located between +4517 and 4662 bp downstream of the *ID3* gene that contains also BRE sites (Nurgazieva et al., 2015). The ECR1 overlaps with a previously described BMP-responsive element in the upstream enhancer of the ID3 gene (nucleotides −3138/−2923 base pairs) (Shepherd et al., 2008), while the ECR2 is a novel SMAD1/5-dependent regulatory element capable of enhancing promoter activity by acting synergistically with ECR1 (Nurgazieva et al., 2015). Reporter plasmids containing either ECR1, ECR2 or both ECR1/ECR2 regions cloned together with an approximately 1-kb fragment of the *ID3* gene promoter were transfected into HEK293 cells and luciferase activity was measured 24 h after transfection. When combined, ECR1 and ECR2 showed a more than additive effect, resulting in a highly significant upregulation of *ID3* promoter activity, particularly in response to BMPs (Fig. 4a). BMP6 was the most effective among the BMPs tested in stimulating *ID3* promoter activity in combination with ECRs, especially in the co-presence of ECR1 and ECR2. Silibinin closely mimicked the ability of dorsomorphin –a pan-BMP signaling inhibitor of all type I BMP receptors (ALK2, ALK3, and ALK6) that blocks BMP-mediated SMAD1/5/8 activation– in preventing BMP6- (and also BMP4-) induced activation of the regulatory sequences of the *ID3* gene. Silibinin partially phenocopied the potent ALK1 inhibitor K02288 to block the BMP9-driven hyperactivation of the ECR1/ECR2-dependent *ID3* promoter activity.

Given the exquisite ability of silibinin to prevent the transcriptional activation of the *ID3* gene promoted by BMP6, the BMP ligand with the highest positive correlation with ID3 in LUAD patients (Fig. 1), we decided to mechanistically investigate the DNA regulatory elements that control silibinin-mediated suppression of ID3 expression driven by BMP6 signal transduction. HEK293 cells transfected with a pGL2-hID3 reporter containing −4432 to +75 base pairs (bp) of the upstream region of the human *ID3* gene, which contains two clusters of SMAD binding sites (i.e., region A and region B), responded significantly to BMP6 (but not to TGFβ), confirming a similar regulation as previously observed with autocrine BMP4 signaling on the endogenous *ID3* gene in ovarian cancer cells (Shepherd et al., 2008; Fig. 4b). The BMP6-induced upregulation of the full-length *ID3* promoter regulatory region was significantly abolished by silibinin treatment. The existence of a BMP6 responsive region required for the ID3 regulatory effects of silibinin was confirmed by a large-scale deletion at the 5′ end to −2728 bp. Deletion of

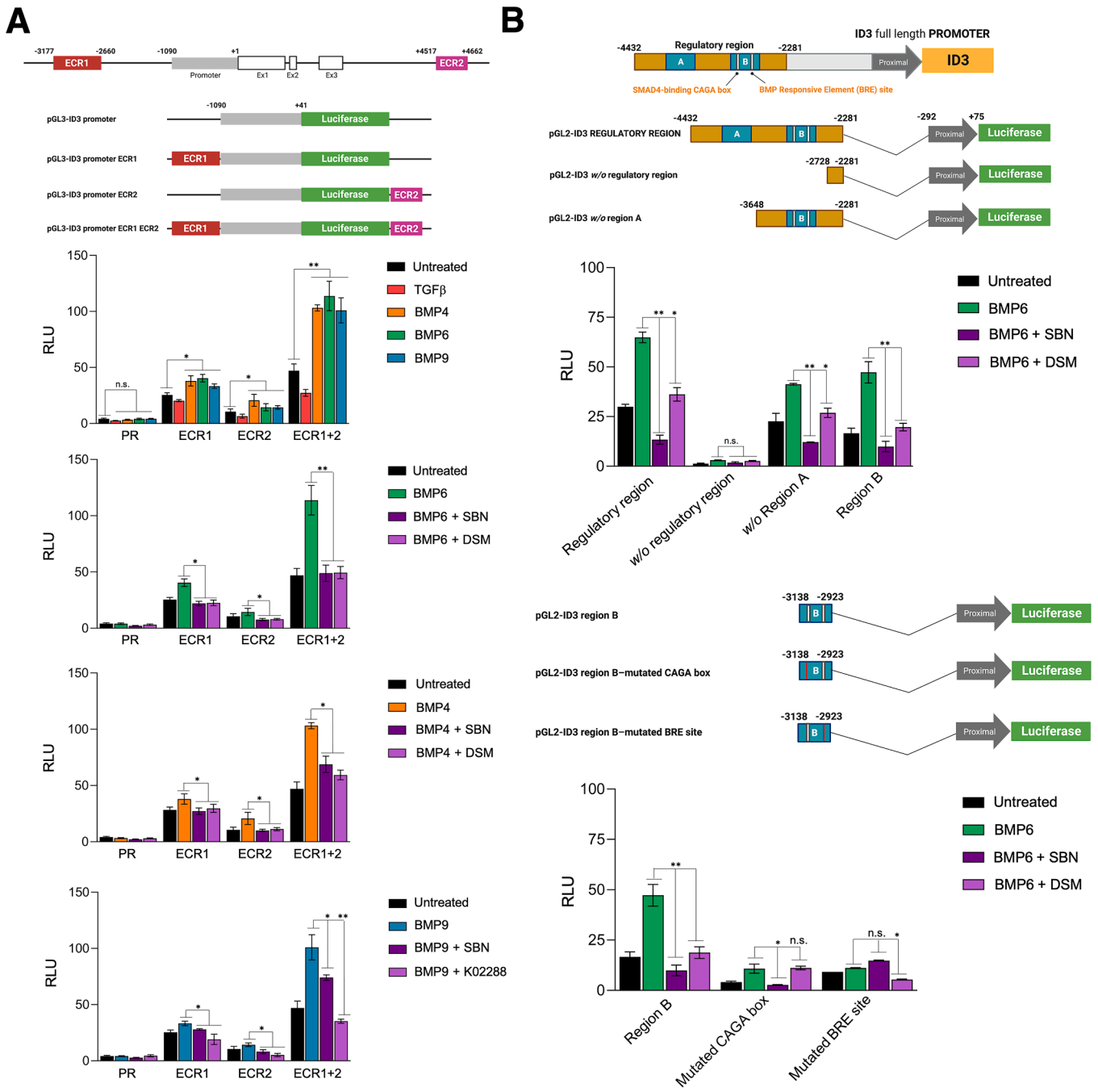

Fig. 4. Identification of the *ID3* gene regulatory regions targeted by silibinin. A. *Top.* Structure of the *ID3* genomic locus showing the enhancers located within the ECR1 and ECR2 regulatory regions and schematic structure of the luciferase plasmid constructs. *Bottom.* Luciferase reporter gene assays of TGFβ-, BMP4-, BMP6-, and BMP9-induced *ID3* promoter and enhancer activities in transfected HEK239T cells cultured in the absence or presence of silibinin (100 μM/l), dorsomorphin (1 μM/l) or K02288 (1 μM/l). Each bar represents the mean ± *S*.D. and the data are representative of three independent experiments performed in triplicate. *$p < 0.05$, ** $p < 0.005$, statistically significant differences. n.s. not significant. B. *Top.* BMP-responsive elements of the upstream ECR1 enhancer region of *ID3* and schematic structure of the luciferase plasmid constructs. *Bottom.* Luciferase reporter gene assays of BMP6-induced *ID3* (ECR1) enhancer activity in transfected HEK239T cells cultured in the absence or presence of silibinin (100 μM/l) or dorsomorphin (1 μM/l). Each bar represents the mean ± S.E. and the data are representative of three independent experiments performed in triplicate. *$p < 0.05$, ** $p < 0.005$, statistically significant differences. DSM, dorsomorphin; SBN, silibinin; RLU, relative light units. n.s. not significant.

the so-called region A including some putative SMAD elements resulted a similar BMP6 responsiveness that was completely abolished in the presence of silibinin. Indeed, the single BMP-responsive ID3 enhancer region (or regulatory region B), including a SMAD4-binding CAGA box and a conserved BMP-responsive element (BRE) site, was sufficient to confer a full BMP6 responsiveness that was exquisitely sensitive to the repressive regulatory effects of silibinin (Fig. 4b). Using reporter constructs with point mutations within the −3138/−2923 region, we observed that while mutation of the CAGA box had no effect on the ability of BMP6 and silibinin to regulate reporter activity, the BMP6 and silibinin responsiveness of the *ID3* enhancer was completely abolished by mutation of the single BRE site that is adjacent to the second CAGA box of the region B (Fig. 4b).

Silibinin is a BMPR receptor inhibitor with significant inhibitory activities against ACVRL1/ALK1, BMPR2 and ALK6

We then investigated whether the above-described ability of silibinin to transcriptionally block the BMP/BMPR-ID3 signaling axis might reflect a direct inhibitory interaction of silibinin with one or various BMPRs. Given that most of the reported inhibitors of the type I BMP receptors work by displacing ATP from the catalytic pocket of the kinase domain, we first performed structural investigations to assess the compatibility of silibinin with the ATP pocket of BMPRs. As silibinin naturally occurs as a 1:1 diastereoisomer mixture of silybins A (7′, 8′ R) and B (7′ S, 8′ S) that configurationally differs in the lignan moiety (Křen et al., 2021; Sciacca et al., 2017), we performed classical molecular docking studies of silybin A and silybin B into the ATP/binding pocket of the seven types I and II BMP receptors (Fig. 5a). When silybin A was used, the resulting binding energies with the docking simulation were in the range of −8.2 to −9.7 kcal/mol. This range was generally higher (from −9.6 to 11.7 kcal/mol) when silybin B was used instead of silybin A. Although it could be argued that these narrow ranges of binding energies largely reflect the high degree of structural similarity between the ATP-binding pocket in the BMP receptors, it was noteworthy that slightly higher binding energies were observed for BMPR2 (−9.465 ± 0.574 [A] versus −11.694 ± 0.730 [B] kcal/mol), ALK6/BMPR1B (−9.646 ± 0.020 [A] versus −11.739 ± 0.640 [B] kcal/mol), and ALK1/ACVRL1 (−9.710 ± 0.492 versus −10.677 ± 0.771 [B] kcal/mol) when the silybin B diastereomer was used in the docking simulations. When the binding affinities were considered in terms of dissociation constants (Kd, which is inversely proportional to the affinity of the BMPR for silibinin), the different behavior predicted for the silibinin diastereoisomers was even more evident. High-affinity Kd values below 100 nM/l were predicted for silybin B against several BMPRs (as low as 5 nM/l for BMPR2 and ALK6/BMPR1B), whereas most Kd values were in the medium to low affinity range (100 nM/l - 2 μM/l) when silybin A was used (Table S2). To better understand these predicted trends, we performed molecular dynamics (MD) simulations for each of the BMP receptor-silybin A/B complexes to account for protein flexibility at the target-binding site during the molecular recognition process, thus allowing to confirm the kinetic stability and to validate the binding poses obtained by docking. To rationalize structure-activity relationships and selectivity profiles of silybin A/B ligands, we first calculated the alchemical binding free energy of silibinin against BMP receptors from the entire MD simulation trajectory of 100 ns (or last 30

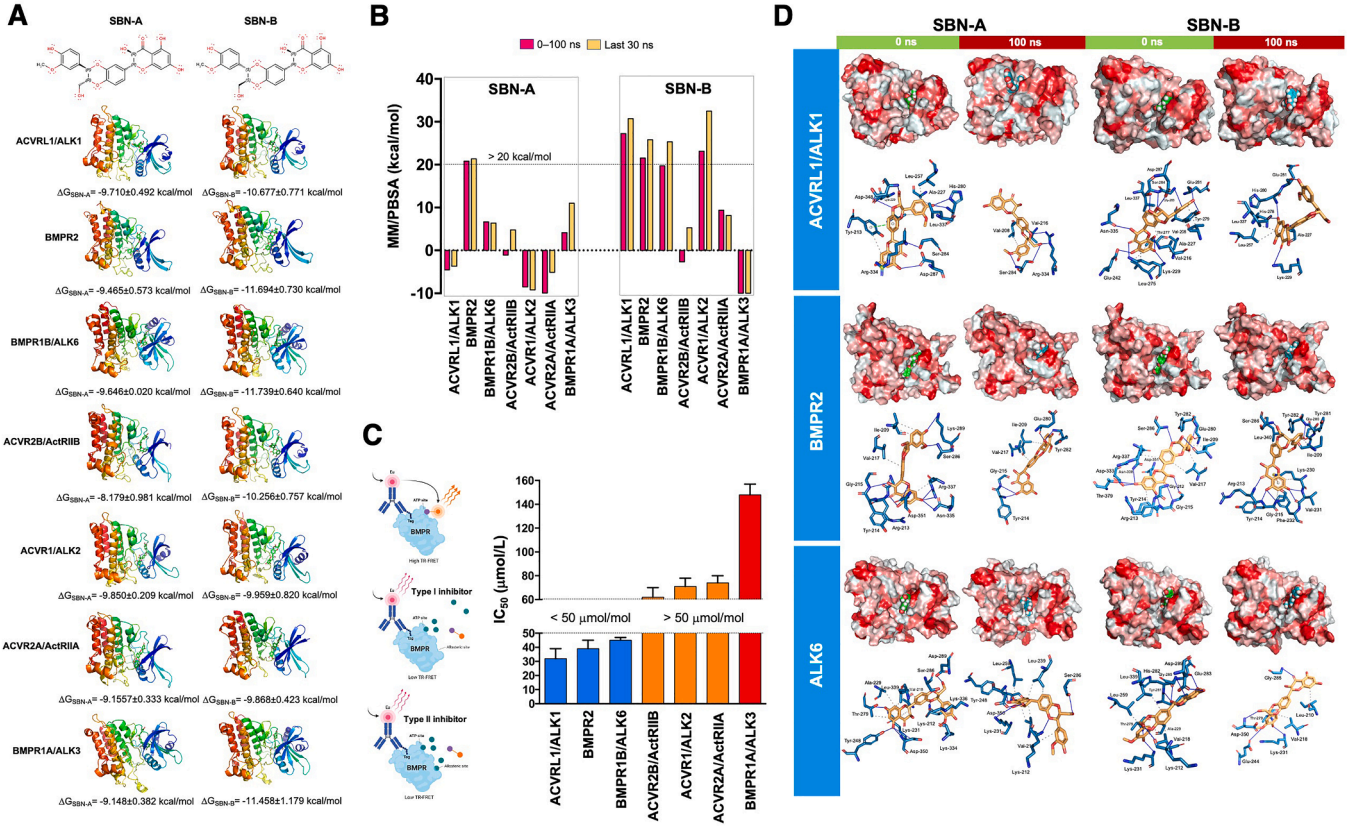

Fig. 5. *In silico* prediction and *in vitro* verification of silibinin as a direct inhibitor of BMPRs. A. Molecular docking simulations and binding energies (ΔG, in kcal/mol) of the silibinin diastereoisomers silybin A (SBN-A) and silybin B (SBN-B) to the ATP-catalytic site of BMPRs. B. Molecular mechanics Poisson-Boltzmann surface area (MM/PBSA) binding energy analyses calculated from the entire trajectory of the 100 ns (or last 30 ns) molecular dynamics (MD) simulations of SBN-A and SBN-B coupled to the catalytic site of BMPRs. C.
Left. Schematic of the LanthaScreen Eu Kinase Binding Assay. Binding of an Alexa Fluor conjugate or "tracer" to a kinase is detected by the addition of an Eu-labeled anti-tag antibody. Binding of the tracer and antibody to a BMPR kinase results in a high level of FRET, whereas displacement of the tracer with a putative BMPR kinase inhibitor results in a loss of FRET. The tracers are based on ATP-competitive kinase inhibitors, making them suitable for the detection of any compound that binds to the BMPR ATP site (type I BMPR kinase inhibitors) and/or to an allosteric site that alters the conformation of the ATP site (type II BMPR kinase inhibitors).
Right. Bar graphs showing the IC_{50} values of silibinin for the ATP-dependent activity of BMPRs calculated from dose-response curves of LanthaScreen Eu kinase binding assays measuring the decreases in emission ratios induced by graded concentrations of silibinin (see "Materials and methods" section). Results are presented as the means (*columns*) ± S.D (*bars*) of three independent experiments performed in duplicate. D. The best positions of SBN-A and SBN-B coupled to the catalytic site of ACVRL1/ALK1, BMPR2, and ALK6 before (0 ns) and after (100 ns) the MD simulations are shown. The protein is plotted as a function of the hydrophobicity of its surface amino acids, and the Na^+ and Cl^- ions have been removed to facilitate visualization. Each inset shows the detailed interactions of the participating amino acids involved and the type of interaction (hydrogen bonds, hydrophilic interactions, salt bridges, Π-stacking, etc.).

ns) using the binding free energy calculations under the molecular mechanics Poisson–Boltzmann surface area (MM/PBSA) approximation (Fig. 5b). Using > 20 kcal/mol as a filtering criterion, only BMPR2 was catalogued as a putative target of silybin A. Four BMP receptors, namely BMPR2, ALK1, ALK2, and ALK6, were cataloged as putative targets of silybin B.

We then used the LanthaScreen Eu kinase binding assay to verify whether silibinin could function as an inhibitor of the ATP-dependent catalytic activity of BMPs. This assay is designed to detect any compound binding to the ATP site, including those binding to the ATP site and adjacent allosteric sites that may be exposed in inactive states of some kinases by monitoring the displacement of an Alexa Fluor 647-labeled "tracer" from the ATP-binding site of an epitope-tagged kinase (here, type II and type I BMP receptors) by a test compound (here, silibinin; Fig. 5c). Such a behavior results in a decreased time-resolved fluorescence resonance energy transfer (FRET) signal. The dose-response curves showed that although the emission ratio was decreased in a dose-dependent manner by graded concentrations of silibinin, the IC_{50} values of silibinin differed up to fivefold between the less sensitive and the more sensitive BMP receptor. Thus, while silibinin concentrations as high as 148 μM/l were required to achieve a half-maximal degree of inhibition in the case of BMPR1A/ALK3, silibinin concentrations as low as 32 μM/l were sufficient to achieve the IC_{50} value against ALK1/ACVRL1. BMPR2, which exclusively binds BMPs but not activin, and ALK6/BMPR1B, which preferentially binds BMP2 and BMP4, also exhibited IC_{50} values below 50 μM/l, while IC_{50}s against ActRIIB/ACVR2B, ALK2/ACVR1, and ActRIIA/ACVR2A ranged from ~60 to 75 μM/l silibinin. Fig. 5D shows the best poses of silybin A and B coupled to the ATP-dependent catalytic cavities of BMPR2, ALK1, and ALK6 to assess the predicted amino acid residues involved in the different diastereoisomeric binding before (0 ns) and after (100 ns) the MD simulation.

Oral treatment with silibinin suppresses ID3 overexpression in vivo

Finally, to provide definitive validation of the translational potential of the ID3 inhibitory effects of silibinin *in vitro* cell models, we evaluated the ability of an oral milk thistle extract formulation enriched (30% *w/w*) with a water-soluble form of silibinin complexed with the amino-sugar meglumine to downregulate ID3 overexpression in an *in vivo* xenograft model of PC-9/ER cells (Cufí et al., 2013a,b). After 35 days of oral treatment with vehicle control, erlotinib (100 mg/kg, 5 days per week), silibinin-meglumine (100 mg/kg, 5 days per week), or silibinin-meglumine plus erlotinib, tumors were collected and snap frozen for the isolation of protein. Remarkably, the extremely high levels of ID3 protein that were observed in PC-9/ER tumors, including those from the erlotinib-treated arm, were drastically down-regulated or completely suppressed in response to systemic treatment with either silibinin-meglumine as a single agent or the combination of erlotinib plus silibinin-meglumine (Fig. 6). Sub-optimal doses of silibinin-meglumine (50 mg/kg, 5 days per week) were still able to significantly reduce ID3 protein expression in PC-9/ER tumors (**Fig. S2**).

Discussion

We report that the milk thistle-derived flavonolignan silibinin is a novel inhibitor of ID3, a transcription factor that is primarily expressed during development to inhibit differentiation, but is aberrantly re-expressed in vascular disease and biologically aggressive carcinomas (Ling et al., 2014; Perez and Felty, 2022). Our discovery that silibinin antagonizes activation of the metastasis-promoting ID3 transcription factor in both the endothelial and tumor cell compartments may be explored as a novel therapeutic approach to interfere with the metastatic dissemination capacity of NSCLC.

NSCLC is a paradigm of human malignancy in which the expression of ID proteins is a strong prognostic biomarker for poor clinical outcome in patients treated with chemoradiotherapy (Castañon et al., 2013; Ponz-Sarvisé et al., 2011). The expression levels of ID1 and ID3 are positively correlated, but the expression level of ID1 is significantly higher and more abundant than that of ID3 in NSCLC (Castañon et al., 2013). In view of the strong sequence similarity and presumed functional redundancy, it could be argued that such an imbalance reflects ID1 activation to functionally compensate for absence of ID3 (O'Brien et al., 2012; Teo et al., 2020). However, it could also reflect a different mechanistic regulation that is related to the different functions of ID1 and ID3 in the promotion of cancer phenotypes (Chaudhary et al., 2001; Perry et al., 2007;). ID3 may play a more important role than ID1 in the regulation of BMP-induced cell growth and survival in lung cancer cells (Langelfeld et al., 2013a). Both ID1 and ID3 downregulate all three cyclin-dependent kinase inhibitors CDKN1B (p27), CDKN1A (p21) and CDKN2B (p16) to accelerate cell proliferation rates. However, ID3 is a preferential regulator of p27 (Garrett-Engele et al., 2007; Chassot et al., 2007), suggesting that ID3 is a more potent therapeutic target than ID1. In spite of the presumed different roles of ID1 and ID3, little is known

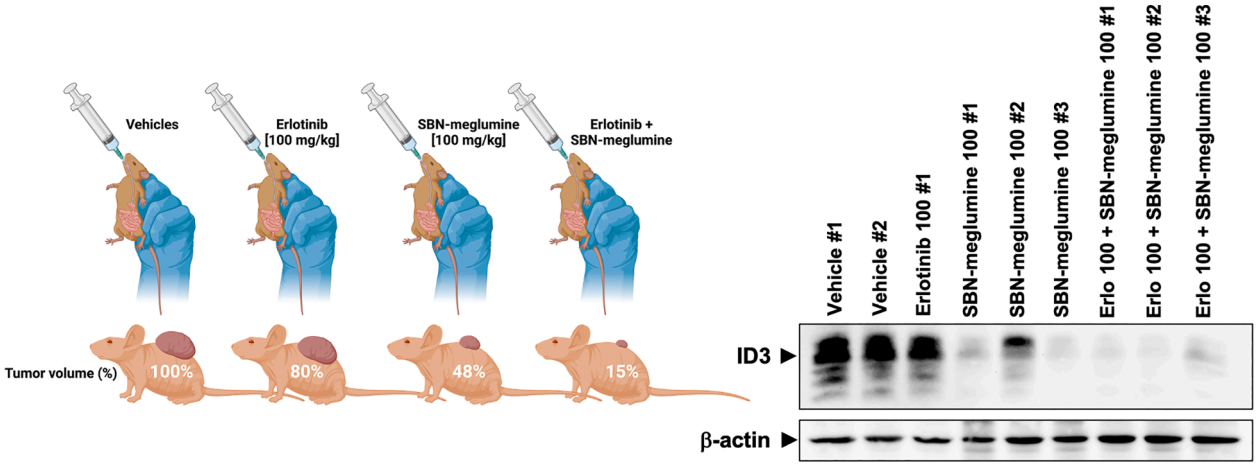

Fig. 6. *In vivo* anti-ID3 activity of a water-soluble form of silibinin. *Top schematic.* Systemic administration by daily oral gavage of a non-toxic, orally active, milk thistle extract rich in silibinin-meglumine, a water-soluble form of silibinin complexed with the excipient amino-sugar meglumine, reduces tumor volumes of erlotinib-refractory PC-9/ER xenografts by approximately 50 %, while a complete abrogation of tumor growth was observed with the co-treatment of erlotinib and silibinin-meglumine (Cufí et al., 2013a;E. b). *Bottom.* Representative immunoblots for ID3 in tumor tissues obtained from PC-9/ER xenograft-bearing mice treated with vehicle control, erlotinib (100 mg/kg, 5 days per week), silibinin-meglumine (100 mg/kg, 5 days per week), or silibinin-meglumine plus erlotinib. Also shown are β-actin loading controls.

about the putative regulators of ID3 in lung cancer patients. In this regard, our current analyses in cohorts of LUAD cancer patients included in the TCGA datasets have established that the expression status of ID3 was significantly correlated with the expression of the BMP ligands BMP6 and BMP2, which are expected to be expressed in the tumor cell compartment of NSCLC and confer poor prognosis by stimulating stem-like phenotypes through the activation of IDs (Langenfeld et al., 2003, 2005, 2006; 2013a,b; Newman et al., 2018). Interestingly, the expression status of *ID3* was also significantly correlated with the expression status of the specialized type I BMP receptor ACVRL1/ALK1 and the co-receptor ENG, which expression pattern is largely restricted to the lung cancer endothelium and closely reflects the vascular nature of ALK1 (Bocci et al., 2019; Mahmoud et al., 2009; Oh et al., 2000). The well-known role of ALK1 as an orchestrator of blood vessels development begins with the high affinity binding to its preferred ligands BMP9 and BMP10 in the vascular compartment (David et al., 2007; de Vinuesa et al., 2016), followed by the recruitment of the constitutively active BMPR2 and the auxiliary receptor ENG. The formation of this complex then triggers the phosphorylation of the ID3-activating transcription factors SMAD1/5/8. The expression of ID3 in lung cancer patients may therefore reflect, at least in part, the activation of biological processes that are under the control of ALK1 in the endothelial compartment to drive tumor angiogenesis and metastatic dissemination (Cunha and Pietras, 2011; Cunha et al., 2010, 2015). Interestingly, endothelial ALK1 expression has recently been implicated in the regulation of gene sets (e.g., "inflammatory response", "interferon-γ", and "IL6/JAK/STAT3") that control immune cell function and infiltration (Bocci et al., 2019). Thus, the expression of ACVRL1/ALK1 is not exclusively associated with the angiogenic process, but extends to other biological processes affecting non-malignant cellular entities in the tumor microenvironment, in particular the immune cells. Previous studies have shown an inverse correlation between ID1 expression and several immune response markers, including PD-L1; in fact, suppression of ID1 has been shown to promote PD-L1 expression on the surface of tumor cells (Baraibar et al., 2020). It may be tempting to suggest that ID1 and ID3 exert complementary but convergent immunoregulatory functions in NSCLC, with the former negatively regulating immune checkpoints in the tumor cell compartment and the latter involved in controlling the immune response downstream of the ALK1-positive endothelial compartment. Nevertheless, the ability of silibinin to function as an ALK1 blocker may warrant further investigation in combination with immunomodulatory drugs to elucidate the therapeutic value of interfering with the BMP9/ALK1/ID3 signaling axis in the endothelial compartment of NSCLC.

ID3 is a key contributor to vessel injury, including microvascular lesions in the lung and brain (Chu et al., 2022; Das and Felty, 2014, 2015; Das et al., 2015). In the lung, *ID3* is a redox-sensitive gene (Felty and Porther, 2008; Mueller et al., 2002) that contributes to the generation of mesenchymal-like, vascular lesion "initiating" ECs that share a molecular stem cell-like signature involving the activation of embryonic transcription factors (OCT4, NANOG, SOX2; Das et al., 2015; Yang et al., 2014) as seen in induced pluripotent stem cells (iPSCs; Hayashi et al., 2016) and tumor-initiating CSCs (Huang et al., 2019). Accordingly, ID3 has been proposed as a molecular risk factor that drives the generation of vascular stem cells under conditions of oxidative stress in the pathogenesis of benign and malignant vascular lesions (Perez and Felty, 2022). In the brain, ID3 overexpression in ECs exposed to oxidative stress conditions leads to increased neovascularization and abnormal vessel sprouting (Das and Felty, 2014). In this scenario, ID3 is a key transcriptional activator of brain angiopathy gene networks, which are mainly involved in the repair of endothelial damage after vascular insults (Perez et al., 2023). Using hCMEC/D3 cells, a stable population of human cerebral microvascular ECs that stably maintains a normal BBB phenotype and is well suited for understanding the response of the brain endothelium to a variety of stimuli (Das and Felty, 2014; J.K. 2015; Das et al., 2015; Weksler et al., 2005), we confirmed the ability of silibinin to molecularly mimic the ALK1 inhibitor K02288 and completely block the inducible activation of the phospho-SMAD1/5-ID3 axis. Our current findings showing that silibinin may function as a novel therapeutic that targets the redox-sensitive transcriptional activation of ID3 to prevent microvascular lesions could be considered as a mechanism by which silibinin-based nutraceuticals clinically prevent the vasogenic edema resulting from BBB breakdown during the growth of established brain metastases (Bosch-Barrera et al., 2016; Priego et al., 2018). Moreover, given that ID3-overexpressing endothelial stem-like cells can direct metastatic cancer cells to cross the BBB (Jayanta et al., 2018), further studies should explore the possibility that anti-ID3 activity of silibinin in brain vascular endothelium may significantly modify both the ability to cross the BBB and the ultimate fate of brain-tropic metastatic cancer cells (i.e., overt BM formation, dormancy, or clearance) involving BBB remodeling.

We observed constitutive and acquired high levels of ID3 expression in NSCLC cell lines with either constitutive or acquired mesenchymal characteristics. Reactivation of fundamental embryonic processes such as EMT is associated with increased cancer cell plasticity, resistance to therapy, reprograming of the local immune response towards immunosuppressive microenvironments, and poor prognosis in several cancers including NSCLC (Byers et al., 2013; Chae et al., 2018; Mak et al., 2016; Thompson et al., 2020). ID3 overexpression in mesenchymal-like NSCLC cells, which may reflect a convergent downstream target of not only autocrine/paracrine BMP signals but also of commonly activated pro-proliferative and pro-oncogenic pathways in cancer cells. The transcriptional suppression of ID3 overexpression by silibinin was certainly notable in EMT-like NSCLCs with acquired resistance to ALK and EGFR TKIs (Cuff et al., 2013a,S. b; Kim et al., 2013; Vazquez-Martin et al., 2013; Verdura et al., 2022). A hyperactive BMP-BMPR-SMAD signaling leading to transcriptional activation of ID3 expression is critical for a successful reprogramming of differentiated cells into iPSCs (Hayashi et al., 2016). In addition, blockade of differentiation transcription factor by ID3 enables the self-renewal response to STAT3 activating signals such as the leukemia inhibitory factor (LIF), a pro-metastatic and immunomodulatory factor of the IL-6 cytokine superfamily (Ying et al., 2003). Given the well-established ability of silibinin to directly block STAT3 activity (Verdura et al., 2018) as an effective mechanism to suppress brain metastasis and therapy-resistant EMT phenotypes (Priego et al., 2018; Verdura et al., 2021), it may be tempting to speculate that the unanticipated capacity of silibinin to inhibit ID3 overexpression could act in synergy with its anti-STAT3 activity to fine-tune the phenotypic plasticity and EMT switching of metastatic cancer cells. Immediate early genes such as *ID3* are rapidly and transiently expressed in response to stressful signals, particularly oxidative damage (Das and Felty, 2014; Mueller et al., 2002). ALK-TKIs such as crizotinib are known to produce excessive endogenous levels of oxidants as a major mechanism of cytotoxicity in various cell types, including cancer cells (Dai et al., 2017; Guo et al., 2021; Yan et al., 2019; Varma and Tiwari, 2021). Our finding that ID3 is transcriptionally activated in response to multi-generation ALK-TKIs (i.e., crizotinib, brigatinib, and erlotinib) may indicate that inducible activation of ID3 is an adaptive antioxidant-mitochondrial response that can be suppressed by silibinin to sensitize NSCLCs to ALK-TKIs.

Aberrant BMP signaling, which leads to the overexpression of ID genes observed in many human cancers, is initiated by one of ~ 20 different extracellular dimeric BMP ligands, typically acting in a paracrine or autocrine manner (Alsamarah et al., 2015; Antebu et al., 2017; Klumpe et al., 2022). BMP ligands signal by binding to three distinct type II receptors (BMPR2, ActR2A/ACVR2A, and ActR2B/ACVR2B), which differ in their ligand and oligomerization partner preferences, and at least four type I receptors commonly known as activin receptor-like kinases (ALK1/ACVRL1, ALK2/ACVR1, ALK3/BMPR1A, and ALK6/BMPR1B) (Nickel and Mueller, 2019; Sanchez-Duffhues et al., 2020). Subsequently, activated BMP type I receptors (ALK1/2/3/6) within the BMP receptor complex phosphorylate the BMP-responsive

SMAD proteins 1 and 5 to facilitate nuclear translocation in complex with the co-SMAD SMAD4, thereby forming DNA sequence-specific transcription factor complexes at the regulatory sequences of BMP-responsive genes including *ID3* (Lewis and Prywes, 2013). Reporter assays were used to determine how silibinin affects the strong positive correlation between certain BMP ligands and ID3 expression in LUAD patients. Transcriptional reporters of the *ID3* regulatory sequences confirmed the ability of silibinin to block BMP-activated *ID3* gene transcription via BMP-responsive elements and SMAD1/5-responsive enhancers located upstream and downstream of intronic enhancers of the *ID3* gene (Nurgazieva et al., 2015; Shepherd et al., 2008). These data raise the possibility that silibinin may reduce endogenous *ID3* mRNA expression by blocking autocrine BMP signaling-induced DNA-protein interactions present at the enhancer elements of the *ID3* gene not only in NSCLC tumor cells themselves but also in the ID3-expressing neovascular endothelium of NSCLC tumors. Specifically, silibinin appears to target ID3 expression by preventing the SMAD complex binding to BRE enhancer elements. Using side-by-side comparisons of *in silico* computational modeling studies with *in vitro* evaluation of kinase selectivity assays, we profiled the ability of silibinin to function as a putative BMP receptor kinase inhibitor to block the BMP/SMAD/ID3 axis upstream. Computational modeling of silibinin diastereoisomers (silybin A and silybin B) (Křen et al., 2021; Sciacca et al., 2017) at the catalytic ATP pocket of the BMPR kinase domains revealed that silibinin possesses a structural basis for the inhibition of specific BMP receptors as a small molecule. Our *in silico* approach suggested a putative role of silibinin stereochemistry in determining the inhibitory potential of silibinin against the kinase activity of BMP receptors, implicating silybin B as the major responsible for the observed BMP/SMAD1/5 signaling-targeted inhibitory effects of the diastereoisomeric silibinin mixture used in cell culture-based experiments. Silybin B, but not silybin A, was predicted to occupy the kinase hinge region of ALK1 in an ATP-mimetic fashion and directly hydrogen-bond to both His280 and the catalytic β3 lysine (Lys229), partially mimicking the inhibitory mechanisms of the ALK1 inhibitors LDN-193,189 and K02288 (Kerr et al., 2015; Sanvitale et al., 2013). Silybin B, but not silybin A, was predicted to interact via hydrogen bonding with the kinase hinge region of BMPR2 and further hydrogen bonding with the Lys230-containing catalytic loop and the phosphate-binding loop (Chaikuad et al., 2019). Both silybin A and silybin B were predicted to occupy the ATP binding pocket of ALK6 involving direct interactions with the catalytic Lys231 (Rooney and Jones, 2021). To confirm the binding potency of silibinin to specific BMPRs, we used a LanthaScreen Eu-based time-resolved FRET-based kinase binding assay to compare the inhibitory potency of silibinin against seven different BMPRs. In vitro screening assays confirmed that silibinin can act as a promiscuous ATP-competitive antagonist of the serine/threonine kinase activity of BMP receptors type I (e.g., ALK1 and ALK6) and type II (e.g., BMPR2) in the tens of micromolar range. Except for ALK2, the predicted binding affinities were in very good agreement with the experimental ones obtained with the natural 1:1 silybin A:silybin B mixture. These computational findings may guide the development of silibinin and/or the next generation of silibinin derivatives as novel BMPR-targeting therapeutics to counter the ID3-driven metastatic phenotype in brain ECs and NSCLC cells.

Our study has several limitations that should be acknowledged. First, silibinin may affect ID3 expression not only by reducing *ID3* gene transcription (through the BMP/BMPR/SMAD pathway carefully dissected here), but also by promoting an imbalance between ID3 protein degradation and synthesis in some scenarios. Curcumin, the major phytochemical component of turmeric that synergistically interacts with silibinin to exert anticancer activity (Montgomery et al., 2016; Sayyed et al., 2022), can trigger the degradation of ID3 by promoting its proteasome-dependent proteolysis (Berse et al., 2004). Further studies should explore whether silibinin can mimic curcumin to target an as yet unknown ID3 ubiquitin ligase and increase the rate of ubiquitin-dependent degradation of ID3. Second, silibinin may reduce ID3 protein synthesis without affecting ID3 protein degradation in NSCLC cells. Silibinin has been shown to block mammalian target of rapamycin (mTOR) signaling to inhibit translation initiation and global protein synthesis associated with reduced levels of eukaryotic initiation factor 4F complex (Garcia-Maceira et al., 2009; Jung et al., 2009; Lin et al., 2009). Whether the partial collapse of polysomes that can be observed in response to silibinin is accompanied by pronounced consequences on the specific translation of the *ID3* mRNA, as has been shown for cyclin D1 (Lin et al., 2009) or HIF-1α (Jung et al., 2009), deserves further investigation. Third, it remains to be determined whether silibinin-driven blockade of ID3 expression causally disrupts several metastatic features in the NSCLC phenotype, including cell spreading/motility, and/or EMT-related drug resistance phenomena.

Systemic administration of an orally active, water-soluble form of silibinin complexed with the amino-acid excipient meglumine (Cufí et al., 2013a,b) was able to completely suppress the extremely high levels of ID3 expression found in EGFR TKI-refractory xenografted tumor tissues in vivo. The corresponding human equivalent dose (HED) for the dose of silibinin used in our in vivo study, which was equivalent to 100 mg/kg mouse body weight, was 8.11 mg/kg. This corresponds to a dose of 486.49 mg of silibinin for a 60-kg individual, an HED that is likely within the dose range that can be achieved in target cancer tissues when using clinically available formulations of silibinin (Bosch-Barrera et al., 2016; Hoh et al., 2006; Kidd, 2009).

Conclusions

As evidence accumulates that ID3 plays a causative role in the spread of metastatic cancer cells to the brain (Das et al., 2022; Das et al., 2018), in the development of adaptive drug resistance to TKI (Sachindra et al., 2017), and in T-cell exhaustion during CAR T-cell immunotherapy (Good et al., 2021), the discovery and development of novel ID3 suppressing agents are urgently needed. We here describe for the first time how the milk thistle flavonolignan silibinin, which has been marketed as a dietary supplement, operates as a novel drug-like inhibitor of *ID3* acting at least in part as a BMP receptor antagonist (Fig. 7). Given the dual capacity of ID3 to drive metastasis by conferring molecular stem cell properties not only in microvascular ECs but also in biologically aggressive subsets of cancer cells, nutraceutical formulations of silibinin with improved bioavailability properties and demonstrated clinical activity could be explored as potential strategy to interfere with the ID3-driven metastatic traits in NSCLC.

Funding

The work in the Menendez laboratory is supported by the Ministerio de Ciencia e Innovación (MCIN, grants PID2019-104055GB-I00 and PID2022-141955OB-I00 to Javier A. Menendez, Plan Nacional de $I+D+i$, funded by the European Regional Development Fund, Spain) and the Emerging Research Group SGR 2021 01,507 to Begoña Martin-Castillo from the Agència de Gestió d'Ajuts Universitaris i de Recerca (AGAUR, Generalitat de Catalunya). Elisabet Cuyàs holds a "Miguel Servet" research contract (CP20/00,003) from the Instituto de Salud Carlos III (Spain) and is supported by the Grant PI22/00,297 (Instituto de Salud Carlos III, Proyectos de $I+D+I$ en Salud, Acción Estratégica en Salud 2021–2023, founded by the European Regional Development Fund, Spain). The work in the Jose A. Encinar laboratory is supported by the Spanish Ministry of Economy and Competitiveness (MINECO, Grant RTI2019–096,724-B-C21) and the Generalitat Valenciana (PROMETEO/2021/059). Eila Serrano-Hervás holds an INVESTIGO research contract (2022 INV-1 00,001, Next Generation Catalunya, Next Generation EU) from the Agència de Gestió d'Ajuts Universitaris i de Recerca (AGAUR, Generalitat de Catalunya). Eduard Teixidor holds a "Rio Hortega" research contract (CM22/00,276, Proyectos de $I+D+I$ en Salud, Acción Estratégica en Salud 2021–2023, founded by the European Regional Development Fund, Spain) from the Instituto de Salud Carlos

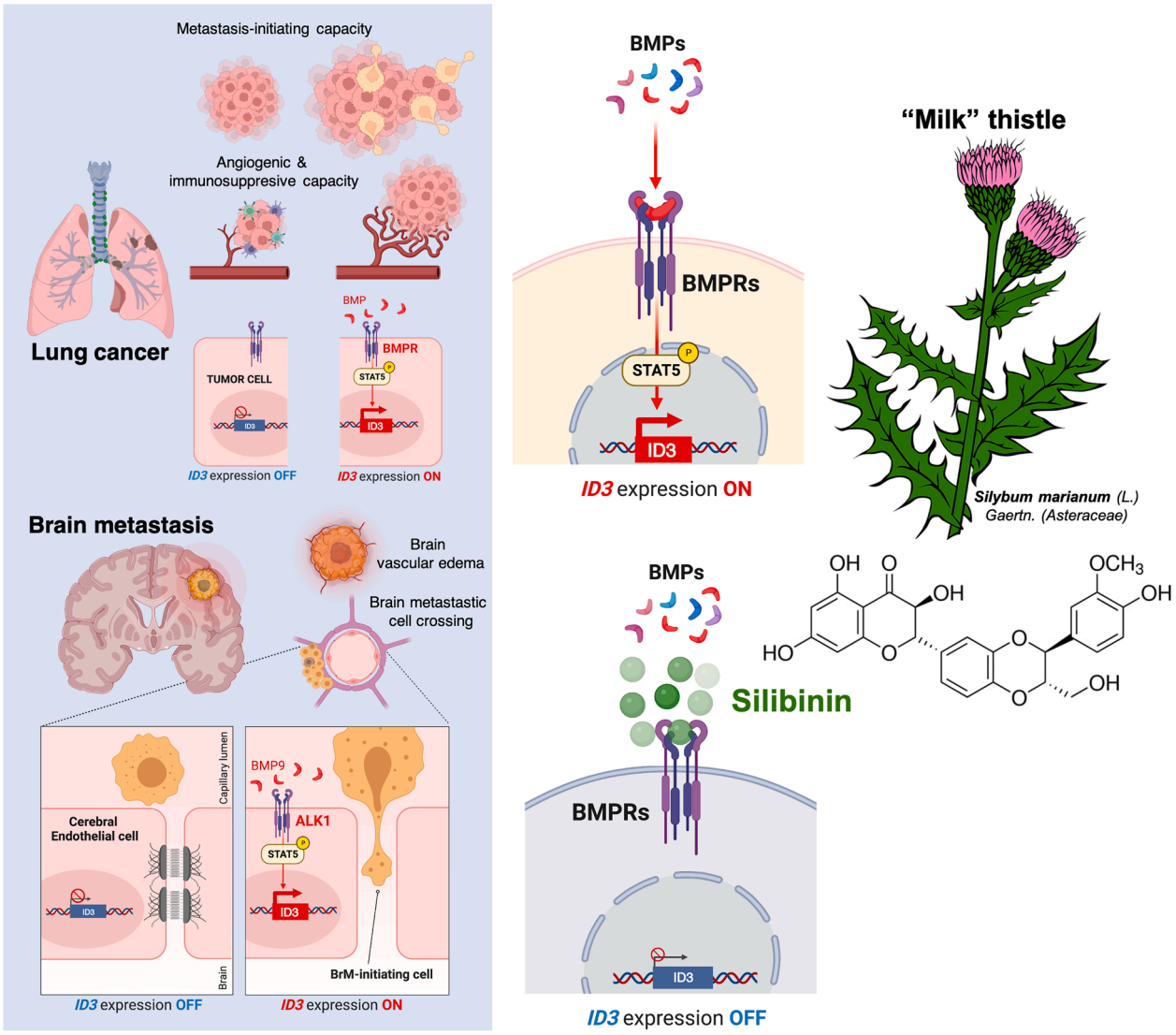

Fig. 7. Silibinin is a novel suppressor of the metastasis-promoting transcription factor ID3. Interfering with the regulatory actions of the metastasis-promoting transcription factor ID3 in primary lung cancer (e.g., metastasis-initiating and angiogenic/immunosuppressive capacity) and lung cancer brain metastasis (e.g., BBB cell crossing, brain vascular edema) may lead to additive or even synergistic anti-metastatic effects. Our research combined bioinformatic analyses, immunoblotting, qRT-PCR, luciferase reporter assays, computational modeling, and kinase assays to elucidate how the flavonolignan silibinin might modulate ID3 expression in endothelial and NSCLC cells. Results from NSCLC patient datasets indicate a strong correlation between ID3 expression and BMP9/ACVRL1/ALK1 and BMP6 levels, with silibinin effectively inhibiting the ALK1-phospho-SMAD1/5-ID3 axis in brain endothelial cells. Notably, silibinin disrupts ID3 expression by targeting BMP-responsive elements within the *ID3* gene enhancers and demonstrates direct inhibition of BMPR kinase activity *in vitro*, with particular potency against ACVRL1/ALK1 and BMPR2. *In vivo,* oral silibinin was found to significantly reduce ID3 overexpression in NSCLC xenograft models. Collectively, these findings altogether suggest that silibinin may serve as a novel therapeutic to reduce the metastatic spread of NSCLC by suppressing ID3 in endothelial and tumor cells.

III (Spain).

Declaration of generative AI and AI-assisted technologies in the writing process

During the preparation of this paper, the authors did not use any AI tool/service or AI-assisted technologies in the writing process.

CRediT authorship contribution statement

Sara Verdura: Methodology, Investigation, Validation, Data curation, Formal analysis, Visualization. **José Antonio Encinar:** Methodology, Investigation, Formal analysis, Visualization, Data curation. **Alexei Gratchev:** Resources, Methodology, Investigation, Visualization. **Àngela Llop-Hernández:** Investigation, Formal analysis, Validation. **Júlia López:** Investigation, Formal analysis, Validation. **Eila Serrano-Hervás:** Investigation, Methodology, Formal analysis, Visualization. **Eduard Teixidor:** Methodology, Investigation, Validation. **Eugeni López-Bonet:** Methodology, Investigation, Visualization. **Begoña Martin-Castillo:** Project administration, Methodology, Investigation. **Vicente Micol:** Conceptualization, Resources, Methodology. **Joaquim Bosch-Barrera:** Conceptualization, Project administration, Supervision, Methodology, Writing – original draft. **Elisabet Cuyàs:** Project administration, Supervision, Resources, Methodology, Formal analysis, Visualization, Writing – original draft. **Javier A. Menendez:** Conceptualization, Project administration, Resources, Supervision, Methodology, Visualization, Writing – original draft, Writing – review & editing.

Declaration of competing interest

The authors declare that they have no known competing financial

interests or personal relationships that could have appeared to influence the work reported in this paper.

Acknowledgments

We are very grateful to Mark W. Nachtigal for kindly providing us with all the pGL2-ID3 reporters, which were instrumental in the functional identification of the elements responsible for silibinin regulation of BMP-stimulated *ID3* gene transcription. We also thank Jin Kyung Rho (Department of Convergence Medicine, Asan Medical Center, University of Ulsan, College of Medicine, Seoul, South Korea) and Jae Cheol Lee (Department of Oncology, Asan Medical Center, University of Ulsan College of Medicine, Seoul, South Korea) for providing us the H2228–H2228/CR (crizotinib-resistant) cell line pair and Daniel B. Costa (Beth Israel Deaconess Medical Center, Harvard Medical Scholl, Boston, MA, USA) for providing the H3122–H3122/CR (crizotinib-resistant) cell line pair. We are grateful to the Servicio de Supercomputación of the University of Granada for allowing us to use the ALBAICIN computer cluster (https://supercomputacion.ugr.es/arquitecturas/albaicin/). We wish to especially thank Santiago Melchor for his kind help and collaboration. We are also grateful to the Cluster of Scientific Computing (http://ccc.umh.es) of the Universidad Miguel Hernández (UMH) for providing computing facilities.

Supplementary materials

Supplementary material associated with this article can be found, in the online version, at doi:10.1016/j.phymed.2024.155493.

References

Alsamarah, A., LaCuran, A.E., Oelschlaeger, P., Hao, J., Luo, Y., 2015. Uncovering molecular bases underlying bone morphogenetic protein receptor inhibitor selectivity. PLoS ONE 10, e0132221.

Anido, J., Sáez-Borderías, A., Gonzàlez-Juncà, A., Rodón, L., Folch, G., Carmona, M.A., Prieto-Sánchez, R.M., Barba, I., Martínez-Sáez, E., Prudkin, L., Cuartas, I., Raventós, C., Martínez-Ricarte, F., Poca, M.A., García-Dorado, D., Lahn, M.M., Yingling, J.M., Rodón, J., Sahuquillo, J., Baselga, J., Seoane, J., 2010. TGF-β receptor inhibitors target the CD44(high)/Id1(high) glioma-initiating cell population in human glioblastoma. Cancer Cell 18, 655–668.

Antebi, Y.E., Linton, J.M., Klumpe, H., Bintu, B., Gong, M., Su, C., McCardell, R., Elowitz, M.B., 2017. Combinatorial signal perception in the BMP pathway. Cell 170, 1184–1196.

Alsina-Sanchís, E., García-Ibáñez, Y., Figueiredo, A.M., Riera-Domingo, C., Figueras, A., Matias-Guiu, X., Casanovas, O., Botella, L.M., Pujana, M.A., Riera-Mestre, A., Graupera, M., Viñals, F., 2018. ALK1 loss results in vascular hyperplasia in mice and humans through PI3K Activation. Arterioscler. Thromb. Vasc. Biol. 38, 1216–1229.

Baraibar, I., Roman, M., Rodríguez-Remírez, M., López, I., Vilalta, A., Guruceaga, E., Ecay, M., Collantes, M., Lozano, T., Alignani, D., Puyalto, A., Oliver, A., Ortiz-Espinosa, S., Moreno, H., Torregrosa, M., Rolfo, C., Caglevic, C., García-Ros, D., Villalba-Esparza, M., De Andrea, C., Vicent, S., Pío, R., Lasarte, J.J., Calvo, A., Ajona, D., Gil-Bazo, I., 2020. Id1 and PD-1 combined blockade impairs tumor growth and survival of *KRAS*-mutant lung cancer by stimulating PD-L1 expression and tumor infiltrating $CD8^+$ T Cells. Cancers (Basel) 12, 3169.

Benezra, R., 2001. Role of Id proteins in embryonic and tumor angiogenesis. Trends Cardiovasc. Med. 11, 237–241.

Berse, M., Bounpheng, M., Huang, X., Christy, B., Pollmann, C., Dubiel, W., 2004. Ubiquitin-dependent degradation of Id1 and Id3 is mediated by the COP9 signalosome. J. Mol. Biol. 343, 361–370.

Bocci, M., Sjölund, J., Kurzejamska, E., Lindgren, D., Marzouka, N.A., Bartoschek, M., Höglund, M., Pietras, K., 2019. Activin receptor-like kinase 1 is associated with immune cell infiltration and regulates CLEC14A transcription in cancer. Angiogenesis 22, 117–131.

Bosch-Barrera, J., Menendez, J.A., 2015. Silibinin and STAT3: a natural way of targeting transcription factors for cancer therapy. Cancer Treat. Rev. 41, 540–546.

Bosch-Barrera, J., Queralt, B., Menendez, J.A., 2017. Targeting STAT3 with silibinin to improve cancer therapeutics. Cancer Treat. Rev. 58, 61–69.

Bosch-Barrera, J., Sais, E., Cañete, N., Marruecos, J., Cuyàs, E., Izquierdo, A., Porta, R., Haro, M., Brunet, J., Pedraza, S., Menendez, J.A., 2016. Response of brain metastasis from lung cancer patients to an oral nutraceutical product containing silibinin. Oncotarget 32006–32014, 2016.

Bosch-Barrera, J., Verdura, S., Ruffinelli, J.C., Carcereny, E., Sais, E., Cuyàs, E., Palmero, R., Lopez-Bonet, E., Hernández-Martínez, A., Oliveras, G., Buxó, M., Izquierdo, A., Morán, T., Nadal, E., Menendez, J.A., 2021. Silibinin suppresses tumor cell-intrinsic resistance to nintedanib and enhances its clinical activity in lung cancer. Cancers (Basel) 13, 4168.

Byers, L.A., Diao, L., Wang, J., Saintigny, P., Girard, L., Peyton, M., Shen, L., Fan, Y., Giri, U., Tumula, P.K., Nilsson, M.B., Gudikote, J., Tran, H., Cardnell, R.J., Bearss, D. J., Warner, S.L., Foulks, J.M., Kanner, S.B., Gandhi, V., Krett, N., Rosen, S.T., Kim, E. S., Herbst, R.S., Blumenschein, G.R., Lee, J.J., Lippman, S.M., Ang, K.K., Mills, G.B., Hong, W.K., Weinstein, J.N., Wistuba, I.I., Coombes, K.R., Minna, J.D., Heymach, J. V., 2013. An epithelial-mesenchymal transition gene signature predicts resistance to EGFR and PI3K inhibitors and identifies Axl as a therapeutic target for overcoming EGFR inhibitor resistance. Clin. Cancer Res. 19, 279–290.

Castañon, E., Bosch-Barrera, J., López, I., Collado, V., Moreno, M., López-Picazo, J.M., Arbea, L., Lozano, M.D., Calvo, A., Gil-Bazo, I., 2013. Id1 and Id3 co-expression correlates with clinical outcome in stage III-N2 non-small cell lung cancer patients treated with definitive chemoradiotherapy. J. Transl. Med. 11, 13.

Chae, Y.K., Chang, S., Ko, T., Anker, J., Agte, S., Iams, W., Choi, W.M., Lee, K., Cruz, M., 2018. Epithelial-mesenchymal transition (EMT) signature is inversely associated with T-cell infiltration in non-small cell lung cancer (NSCLC). Sci. Rep. 8, 2918.

Chaikuad, A., Thangaratnarajah, C., von Delft, F., Bullock, A.N., 2019. Structural consequences of BMPR2 kinase domain mutations causing pulmonary arterial hypertension. Sci. Rep. 9, 18351.

Chassot, A.A., Turchi, L., Virolle, T., Fitsialos, G., Batoz, M., Deckert, M., Dulic, V., Meneguzzi, G., Buscà, R., Ponzio, G., 2007. Id3 is a novel regulator of p27kip1 mRNA in early G1 phase and is required for cell-cycle progression. Oncogene 26, 5772–5783.

Chaudhary, J., Johnson, J., Kim, G., Skinner, M.K., 2001. Hormonal regulation and differential actions of the helix-loop-helix transcriptional inhibitors of differentiation (Id1, Id2, Id3, and Id4) in Sertoli cells. Endocrinology 142, 1727–1736.

Chen, H., Nio, K., Yamashita, T., Okada, H., Li, R., Suda, T., Li, Y., Doan, P.T.B., Seki, A., Nakagawa, H., Toyama, T., Terashima, T., Iida, N., Shimakami, T., Takatori, H., Kawaguchi, K., Sakai, Y., Yamashita, T., Mizukoshi, E., Honda, M., Kaneko, S., 2021. BMP9-ID1 signaling promotes EpCAM-positive cancer stem cell properties in hepatocellular carcinoma. Mol. Oncol. 15, 2203–2218.

Chu, Y.H., Lin, J.D., Nath, S., Schachtrup, C., 2022. Id proteins: emerging roles in CNS disease and targets for modifying neural stem cell behavior. Cell Tissue Res. 387, 433–449.

Cufí, S., Bonavia, R., Vazquez-Martin, A., Corominas-Faja, B., Oliveras-Ferraros, C., Cuyàs, E., Martin-Castillo, B., Barrajón-Catalán, E., Visa, J., Segura-Carretero, A., Bosch-Barrera, J., Joven, J., Micol, V., Menendez, J.A., 2013a. Silibinin meglumine, a water-soluble form of milk thistle silymarin, is an orally active anti-cancer agent that impedes the epithelial-to-mesenchymal transition (EMT) in EGFR-mutant non-small-cell lung carcinoma cells. Food Chem. Toxicol. 60, 360–368.

Cufí, S., Bonavia, R., Vazquez-Martin, A., Oliveras-Ferraros, C., Corominas-Faja, B., Cuyàs, E., Martin-Castillo, B., Barrajón-Catalán, E., Visa, J., Segura-Carretero, A., Joven, J., Bosch-Barrera, J., Micol, V., Menendez, J.A., 2013b. Silibinin suppresses EMT-driven erlotinib resistance by reversing the high miR-21/low miR-200c signature in vivo. Sci. Rep. 3, 2459.

Cunha, S.I., Bocci, M., Lövrot, J., Eleftheriou, N., Roswall, P., Cordero, E., Lindström, L., Bartoschek, M., Haller, B.K., Pearsall, R.S., Mulivor, A.W., Kumar, R., Larsson, C., Bergh, J., Pietras, K., 2015. Endothelial ALK1 is a therapeutic target to block metastatic dissemination of breast cancer. Cancer Res. 75, 2445–2456.

Cunha, S.I., Pardali, E., Thorikay, M., Anderberg, C., Hawinkels, L., Goumans, M.J., Seehra, J., Heldin, C.H., ten Dijke, P., Pietras, K., 2010. Genetic and pharmacological targeting of activin receptor-like kinase 1 impairs tumor growth and angiogenesis. J. Exp. Med. 207, 85–100.

Cunha, S.I., Pietras, K., 2011. ALK1 as an emerging target for antiangiogenic therapy of cancer. Blood 117, 6999–7006.

Cuyàs, E., Verdura, S., Micol, V., Joven, J., Bosch-Barrera, J., Encinar, J.A., Menendez, J. A., 2019. Revisiting silibinin as a novobiocin-like Hsp90 C-terminal inhibitor: computational modeling and experimental validation. Food Chem. Toxicol. 132, 110645.

Dai, X., Guo, G., Zou, P., Cui, R., Chen, W., Chen, X., Yin, C., He, W., Vinothkumar, R., Yang, F., Zhang, X., Liang, G., 2017. (S)-crizotinib induces apoptosis in human non-small cell lung cancer cells by activating ROS independent of MTH1. J. Exp. Clin. Cancer Res. 36, 120.

Das, J.K., Deoraj, A., Roy, D., Felty, Q., 2022. Brain infiltration of breast cancer stem cells is facilitated by paracrine signaling by inhibitor of differentiation 3 to nuclear respiratory factor 1. J. Cancer Res. Clin. Oncol. 148, 2881–2891.

Das, J.K., Felty, Q., 2015. Microvascular lesions by estrogen-induced ID3: its implications in cerebral and cardiorenal vascular disease. J. Mol. Neurosci. 55, 618–631.

Das, J.K., Felty, Q., 2014. PCB153-induced overexpression of ID3 contributes to the development of microvascular lesions. PLoS ONE 9, e104159.

Das, J.K., Voelkel, N.F., Felty, Q., 2015. ID3 contributes to the acquisition of molecular stem cell-like signature in microvascular endothelial cells: its implication for understanding microvascular diseases. Microvasc. Res. 98, 126–138.

David, L., Mallet, C., Mazerbourg, S., Feige, J.J., Bailly, S., 2007. Identification of BMP9 and BMP10 as functional activators of the orphan activin receptor-like kinase 1 (ALK1) in endothelial cells. Blood 109, 1953–1961.

de Vinuesa, A.G., Bocci, M., Pietras, K., Ten Dijke, P., 2016. Targeting tumour vasculature by inhibiting activin receptor-like kinase (ALK)1 function. Biochem. Soc. Trans. 44, 1142–1149.

Deep, G., Agarwal, R., 2010. Antimetastatic efficacy of silibinin: molecular mechanisms and therapeutic potential against cancer. Cancer Metastasis Rev. 29, 447–463.

Deep, G., Agarwal, R., 2013. Targeting tumor microenvironment with silibinin: promise and potential for a translational cancer chemopreventive strategy. Curr. Cancer Drug Targets 13, 486–499.

Deep, G., Kumar, R., Nambiar, D.K., Jain, A.K., Ramteke, A.M., Serkova, N.J., Agarwal, C., Agarwal, R., 2017. Silibinin inhibits hypoxia-induced HIF-1α-mediated

signaling, angiogenesis and lipogenesis in prostate cancer cells: in vitro evidence and in vivo functional imaging and metabolomics. Mol. Carcinog. 56, 833–848.
Encinar, J.A., Menendez, J.A., 2020. Potential Drugs targeting early innate immune evasion of sars-coronavirus 2 via 2′-O-methylation of viral RNA. Viruses 12, 525.
Felty, Q., Porther, N., 2008. Estrogen-induced redox sensitive Id3 signaling controls the growth of vascular cells. Atherosclerosis 198, 12–21.
Gao, D., Nolan, D.J., Mellick, A.S., Bambino, K., McDonnell, K., Mittal, V., 2008. Endothelial progenitor cells control the angiogenic switch in mouse lung metastasis. Science 319, 195–198.
García-Maceira, P., Mateo, J., 2009. Silibinin inhibits hypoxia-inducible factor-1alpha and mTOR/p70S6K/4E-BP1 signalling pathway in human cervical and hepatoma cancer cells: implications for anticancer therapy. Oncogene 28, 313–324.
Garrett-Engele, C.M., Tasch, M.A., Hwang, H.C., Fero, M.L., Perlmutter, R.M., Clurman, B.E., Roberts, J.M., 2007. A mechanism misregulating p27 in tumors discovered in a functional genomic screen. PLoS Genet. 3, e219.
Good, C.R., Aznar, M.A., Kuramitsu, S., Samareh, P., Agarwal, S., Donahue, G., Ishiyama, K., Wellhausen, N., Rennels, A.K., Ma, Y., Tian, L., Guedan, S., Alexander, K.A., Zhang, Z., Rommel, P.C., Singh, N., Glastad, K.M., Richardson, M. W., Watanabe, K., Tanyi, J.L., O'Hara, M.H., Ruella, M., Lacey, S.F., Moon, E.K., Schuster, S.J., Albelda, S.M., Lanier, L.L., Young, R.M., Berger, S.L., June, C.H., 2021. An NK-like CAR T cell transition in CAR T cell dysfunction. Cell 184, 6081–6100.
Guo, L., Gong, H., Tang, T.L., Zhang, B.K., Zhang, L.Y., Yan, M., 2021. Crizotinib and sunitinib induce hepatotoxicity and mitochondrial apoptosis in L02 Cells via ROS and Nrf2 signaling pathway. Front. Pharmacol. 12, 620934.
Gupta, G.P., Perk, J., Acharyya, S., de Candia, P., Mittal, V., Todorova-Manova, K., Gerald, W.L., Brogi, E., Benezra, R., Massagué, J., 2007. ID genes mediate tumor reinitiation during breast cancer lung metastasis. Proc. Natl. Acad. Sci. USA 104, 19506–19511.
Hayashi, Y., Hsiao, E.C., Sami, S., Lancero, M., Schlieve, C.R., Nguyen, T., Yano, K., Nagahashi, A., Ikeya, M., Matsumoto, Y., Nishimura, K., Fukuda, A., Hisatake, K., Tomoda, K., Asaka, I., Toguchida, J., Conklin, B.R., Yamanaka, S., 2016. BMP-SMAD-ID promotes reprogramming to pluripotency by inhibiting p16/INK4A-dependent senescence. Proc. Natl. Acad. Sci. USA 113, 13057–13062.
Hiepen, C., Jatzlau, J., Hildebrandt, S., Kampfrath, B., Goktas, M., Murgai, A., Cuellar Camacho, J.L., Haag, R., Ruppert, C., Sengle, G., Cavalcanti-Adam, E.A., Blank, K.G., Knaus, P., 2019. BMPR2 acts as a gatekeeper to protect endothelial cells from increased TGFβ responses and altered cell mechanics. PLoS Biol. 17, e3000557.
Hiepen, C., Mendez, P.L., Knaus, P., 2020. It takes two to tango: endothelial TGFβ/BMP signaling crosstalk with mechanobiology. Cells 9, 1965.
Hoh, C., Boocock, D., Marczylo, T., Singh, R., Berry, D.P., Dennison, A.R., Hemingway, D., Miller, A., West, K., Euden, S., Garcea, G., Farmer, P.B., Steward, W. P., Gescher, A.J., 2006. Pilot study of oral silibinin, a putative chemopreventive agent, in colorectal cancer patients: silibinin levels in plasma, colorectum, and liver and their pharmacodynamic consequences. Clin. Cancer Res. 12, 2944–2950.
Hollnagel, A., Oehlmann, V., Heymer, J., Rüther, U., Nordheim, A., 1999. Id genes are direct targets of bone morphogenetic protein induction in embryonic stem cells. J. Biol. Chem. 274, 19838–19845.
Huang, L., Cai, J., Guo, H., Gu, J., Tong, Y., Qiu, B., Wang, C., Li, M., Xia, L., Zhang, J., Wu, H., Kong, X., Xia, Q., 2019. ID3 Promotes Stem Cell Features and Predicts Chemotherapeutic Response of Intrahepatic Cholangiocarcinoma. Hepatology 69, 1995–2012.
Iavarone, A., Lasorella, A., 2006. ID proteins as targets in cancer and tools in neurobiology. Trends Mol. Med. 12, 588–594.
Das, J.K., Doke, M., Deoraj, A., Felty, Q., Roy, D., 2018. Exosomal ID3 is pro-metastatic through guiding NRF1-induced breast cancer stem cells across the blood-brain-barrier. In: Cancer Res., 78, p. 1128.
Jung, H.J., Park, J.W., Lee, J.S., Lee, S.R., Jang, B.C., Suh, S.I., Suh, M.H., Baek, W.K., 2009. Silibinin inhibits expression of HIF-1alpha through suppression of protein translation in prostate cancer cells. Biochem. Biophys. Res. Commun. 390, 71–76.
Ke, J., Wu, R., Chen, Y., Abba, M.L., 2018. Inhibitor of DNA binding proteins: implications in human cancer progression and metastasis. Am. J. Transl. Res. 10, 3887–3910.
Kerr, G., Sheldon, H., Chaikuad, A., Alfano, I., von Delft, F., Bullock, A.N., Harris, A.L., 2015. A small molecule targeting ALK1 prevents Notch cooperativity and inhibits functional angiogenesis. Angiogenesis 18, 209–217.
Kidd, P.M., 2009. Bioavailability and activity of phytosome complexes from botanical polyphenols: the silymarin, curcumin, green tea, and grape seed extracts. Altern. Med. Rev. 14, 226–246.
Kim, H.R., Kim, W.S., Choi, Y.J., Choi, C.M., Rho, J.K., Lee, J.C., 2013. Epithelial-mesenchymal transition leads to crizotinib resistance in H2228 lung cancer cells with EML4-ALK translocation. Mol. Oncol. 7, 1093–1102.
Klumpe, H.E., Langley, M.A., Linton, J.M., Su, C.J., Antebi, Y.E., Elowitz, M.B., 2022. The context-dependent, combinatorial logic of BMP signaling. Cell Syst 13, 388–407.
Kowanetz, M., Valcourt, U., Bergström, R., Heldin, C.H., Moustakas, A., 2004. Id2 and Id3 define the potency of cell proliferation and differentiation responses to transforming growth factor beta and bone morphogenetic protein. Mol. Cell. Biol. 24, 4241–4254.
Křen, V., 2021. Chirality matters: biological activity of optically pure silybin and its congeners. Int. J. Mol. Sci. 22, 7885.
Langenfeld, E., Deen, M., Zachariah, E., Langenfeld, J., 2013a. Small molecule antagonist of the bone morphogenetic protein type I receptors suppresses growth and expression of Id1 and Id3 in lung cancer cells expressing Oct4 or nestin. Mol. Cancer. 12, 129.
Langenfeld, E., Hong, C.C., Lanke, G., Langenfeld, J., 2013b. Bone morphogenetic protein type I receptor antagonists decrease growth and induce cell death of lung cancer cell lines. PLoS ONE 8, e61256.
Langenfeld, E.M., Bojnowski, J., Perone, J., Langenfeld, J., 2005. Expression of bone morphogenetic proteins in human lung carcinomas. Ann. Thorac. Surg. 80, 1028–1032.
Langenfeld, E.M., Calvano, S.E., Abou-Nukta, F., Lowry, S.F., Amenta, P., Langenfeld, J., 2003. The mature bone morphogenetic protein-2 is aberrantly expressed in non-small cell lung carcinomas and stimulates tumor growth of A549 cells. Carcinogenesis 24, 1445–1454.
Langenfeld, E.M., Kong, Y., Langenfeld, J., 2006. Bone morphogenetic protein 2 stimulation of tumor growth involves the activation of Smad-1/5. Oncogene 25, 685–692.
Lasorella, A., Benezra, R., Iavarone, A., 2014. The ID proteins: master regulators of cancer stem cells and tumour aggressiveness. Nat. Rev. Cancer 14, 77–91.
Lee, K.T., Lee, Y.W., Lee, J.K., Choi, S.H., Rhee, J.C., Paik, S.S., Kong, G., 2004. Overexpression of Id-1 is significantly associated with tumour angiogenesis in human pancreas cancers. Br. J. Cancer 90, 1198–1203.
Lewis, T.C., Prywes, R., 2013. Serum regulation of Id1 expression by a BMP pathway and BMP responsive element. Biochim. Biophys. Acta 1829, 1147–1159.
Lin, C.J., Sukarieh, R., Pelletier, J., 2009. Silibinin inhibits translation initiation: implications for anticancer therapy. Mol. Cancer Ther. 8, 1606–1612.
Ling, F., Kang, B., Sun, X.H., 2014. Id proteins: small molecules, mighty regulators. Curr. Top. Dev. Biol. 110, 189–216.
Lyden, D., Young, A.Z., Zagzag, D., Yan, W., Gerald, W., O'Reilly, R., Bader, B.L., Hynes, R.O., Zhuang, Y., Manova, K., Benezra, R., 1999. Id1 and Id3 are required for neurogenesis, angiogenesis and vascularization of tumour xenografts. Nature 401, 670–677.
Mahmoud, M., Borthwick, G.M., Hislop, A.A., Arthur, H.M., 2009. Endoglin and activin receptor-like-kinase 1 are co-expressed in the distal vessels of the lung: implications for two familial vascular dysplasias, HHT and PAH. Lab. Invest. 89, 15–25.
Mak, M.P., Tong, P., Diao, L., Cardnell, R.J., Gibbons, D.L., William, W.N., Skoulidis, F., Parra, E.R., Rodriguez-Canales, J., Wistuba, I.I., Heymach, J.V., Weinstein, J.N., Coombes, K.R., Wang, J., Byers, L.A., 2016. A patient-derived, pan-cancer emt signature identifies global molecular alterations and immune target enrichment following epithelial-to-mesenchymal transition. Clin. Cancer Res. 22, 609–620.
Mateen, S., Raina, K., Agarwal, R., 2013. Chemopreventive and anti-cancer efficacy of silibinin against growth and progression of lung cancer. Nutr. Cancer 65 (Suppl 1), 3–11.
Maw, M.K., Fujimoto, J., Tamaya, T., 2008. Expression of the inhibitor of DNA-binding (ID)-1 protein as an angiogenic mediator in tumour advancement of uterine cervical cancers. Br. J. Cancer 99, 1557–1563.
Mern, D.S., Hasskarl, J., Burwinkel, B., 2010. Inhibition of Id proteins by a peptide aptamer induces cell-cycle arrest and apoptosis in ovarian cancer cells. Br. J. Cancer 103, 1237–1244.
Mirzaaghaei, S., Foroughmand, A.M., Saki, G., Shafiei, M., 2019. Combination of Epigallocatechin-3-gallate and silibinin: a novel approach for targeting both tumor and endothelial cells. ACS Omega 4, 8421–8430.
Montgomery, A., Adeyeni, T., San, K., Heuertz, R.M., Ezekiel, U.R., 2016. Curcumin sensitizes silymarin to exert synergistic anticancer activity in colon cancer cells. J. Cancer. 7, 1250–1257.
Mueller, C., Baudler, S., Welzel, H., Böhm, M., Nickenig, G., 2002. Identification of a novel redox-sensitive gene, Id3, which mediates angiotensin II-induced cell growth. Circulation 105, 2423–2428.
Nair, R., Teo, W.S., Mittal, V., Swarbrick, A., 2014. ID proteins regulate diverse aspects of cancer progression and provide novel therapeutic opportunities. Mol. Ther. 22, 1407–1415.
Newman, J.H., Augeri, D.J., NeMoyer, R., Malhotra, J., Langenfeld, E., Chesson, C.B., Dobias, N.S., Lee, M.J., Tarabichi, S., Jhawar, S.R., Bommareddy, P.K., Marshall, S., Sadimin, E.T., Kerrigan, J.E., Goedken, M., Minerowicz, C., Jabbour, S.K., Li, S., Carayannopolous, M.O., Zloza, A., Langenfeld, J., 2018. Novel bone morphogenetic protein receptor inhibitor JL5 suppresses tumor cell survival signaling and induces regression of human lung cancer. Oncogene 37, 3672–3685.
Nickel, J., Mueller, T.D., 2019. Specification of BMP Signaling. Cells 8, 1579.
Niola, F., Zhao, X., Singh, D., Castano, A., Sullivan, R., Lauria, M., Nam, H.S., Zhuang, Y., Benezra, R., Di Bernardo, D., Iavarone, A., Lasorella, A., 2012. Id proteins synchronize stemness and anchorage to the niche of neural stem cells. Nat. Cell. Biol. 14, 477–487.
Nurgazieva, D., Mickley, A., Moganti, K., Ming, W., Ovsyi, I., Popova, A., Sachindra, Awad K., Wang, N., Bieback, K., Goerdt, S., Kzhyshkowska, J., Gratchev, A., 2015. TGF-β1, but not bone morphogenetic proteins, activates Smad1/5 pathway in primary human macrophages and induces expression of proatherogenic genes. J. Immunol. 194, 709–718.
O'Brien, C.A., Kreso, A., Ryan, P., Hermans, K.G., Gibson, L., Wang, Y., Tsatsanis, A., Gallinger, S., Dick, J.E., 2012. ID1 and ID3 regulate the self-renewal capacity of human colon cancer-initiating cells through p21. Cancer Cell 21, 777–792.
Oh, S.P., Seki, T., Goss, K.A., Imamura, T., Yi, Y., Donahoe, P.K., Li, L., Miyazono, K., ten Dijke, P., Kim, S., Li, E., 2000. Activin receptor-like kinase 1 modulates transforming growth factor-beta 1 signaling in the regulation of angiogenesis. Proc. Natl. Acad. Sci. USA 97, 2626–2631.
Perez, C.M., Felty, Q., 2022. Molecular basis of the association between transcription regulators nuclear respiratory factor 1 and inhibitor of DNA binding protein 3 and the development of microvascular lesions. Microvasc. Res. 141, 104337.
Perez, C.M., Gong, Z., Yoo, C., Roy, D., Deoraj, A., Felty, Q., 2023. Inhibitor of DNA binding protein 3 (ID3) and nuclear respiratory factor 1 (NRF1) mediated transcriptional gene signatures are associated with the severity of cerebral amyloid

angiopathy. Mol. Neurobiol. https://doi.org/10.1007/s12035-023-03541-2, 2023 Sep 5.
Perk, J., Iavarone, A., Benezra, R., 2005. Id family of helix-loop-helix proteins in cancer. Nat. Rev. Cancer 5, 603–614.
Perry, S.S., Zhao, Y., Nie, L., Cochrane, S.W., Huang, Z., Sun, X.H., 2007. Id1, but not Id3, directs long-term repopulating hematopoietic stem-cell maintenance. Blood 110, 2351–2360.
Ponz-Sarvisé, M., Nguewa, P.A., Pajares, M.J., Agorreta, J., Lozano, M.D., Redrado, M., Pio, R., Behrens, C., Wistuba, I.I., García-Franco, C.E., García-Foncillas, J., Montuenga, L.M., Calvo, A., Gil-Bazo, I., 2011. Inhibitor of differentiation-1 as a novel prognostic factor in NSCLC patients with adenocarcinoma histology and its potential contribution to therapy resistance. Clin. Cancer Res. 17, 4155–4166.
Priego, N., Valiente, M., 2019. The Potential of astrocytes as immune modulators in brain tumors. Front. Immunol. 10, 1314.
Priego, N., Zhu, L., Monteiro, C., Mulders, M., Wasilewski, D., Bindeman, W., Doglio, L., Martínez, L., Martínez-Saez, E., Ramón y Cajal, S., Megías, D., Hernández-Encinas, E., Blanco-Aparicio, C., Martínez, L., Zarzuela, E., Muñoz, J., Fustero-Torre, C., Piñeiro-Yáñez, E., Hernández-Laín, A., Bertero, L., Poli, V., Sanchez-Martinez, M., Menendez, J.A., Soffietti, R., Bosch-Barrera, J., Valiente, M., 2018. STAT3 labels a subpopulation of reactive astrocytes required for brain metastasis. Nat. Med. 24, 1024–1035.
Richter, J., Schlesner, M., Hoffmann, S., Kreuz, M., Leich, E., Burkhardt, B., Rosolowski, M., Ammerpohl, O., Wagener, R., Bernhart, S.H., Lenze, D., Szczepanowski, M., Paulsen, M., Lipinski, S., Russell, R.B., Adam-Klages, S., Apic, G., Claviez, A., Hasenclever, D., Hovestadt, V., Hornig, N., Korbel, J.O., Kube, D., Langenberger, D., Lawerenz, C., Lisfeld, J., Meyer, K., Picelli, S., Pischimarov, J., Radlwimmer, B., Rausch, T., Rohde, M., Schilhabel, M., Scholtysik, R., Spang, R., Trautmann, H., Zenz, T., Borkhardt, A., Drexler, H.G., Möller, P., MacLeod, R.A., Pott, C., Schreiber, S., Trümper, L., Loeffler, M., Stadler, P.F., Lichter, P., Eils, R., Küppers, R., Hummel, M., Klapper, W., Rosenstiel, P., Rosenwald, A., Brors, B., Siebert, R., 2012. Recurrent mutation of the ID3 gene in Burkitt lymphoma identified by integrated genome, exome and transcriptome sequencing. Nat. Genet. 44, 1316–1320.
Rooney, L., Jones, C., 2021. Recent advances in ALK2 inhibitors. ACS Omega 6, 20729–20734.
Roschger, C., Cabrele, C., 2017. The Id-protein family in developmental and cancer-associated pathways. Cell. Commun. Signal. 15, 7.
Sachindra, Larribère L., Novak, D., Wu, H., Hüser, L., Granados, K., Orouji, E., Utikal, J., 2017. New role of ID3 in melanoma adaptive drug-resistance. Oncotarget 8, 110166–110175.
Sanchez-Duffhues, G., Williams, E., Goumans, M.J., Heldin, C.H., Ten Dijke, P., 2020. Bone morphogenetic protein receptors: structure, function and targeting by selective small molecule kinase inhibitors. Bone 138, 115472.
Sanvitale, C.E., Kerr, G., Chaikuad, A., Ramel, M.C., Mohedas, A.H., Reichert, S., Wang, Y., Triffitt, J.T., Cuny, G.D., Yu, P.B., Hill, C.S., Bullock, A.N., 2013. A new class of small molecule inhibitor of BMP signaling. PLoS ONE 8, e62721.
Sayyed, A., Heuertz, R., Ezekiel, U.R., 2022. Curcumin, but not its degradation products, in combination with silibinin is primarily responsible for the inhibition of colon cancer cell proliferation. MicroPubl. Biol. https://doi.org/10.17912/micropub.biology.000617, 2022.
Schindl, M., Schoppmann, S.F., Ströbel, T., Heinzl, H., Leisser, C., Horvat, R., Birner, P., 2003. Level of Id-1 protein expression correlates with poor differentiation, enhanced malignant potential, and more aggressive clinical behavior of epithelial ovarian tumors. Clin. Cancer Res. 9, 779–785.
Schliekelman, M.J., Taguchi, A., Zhu, J., Dai, X., Rodriguez, J., Celiktas, M., Zhang, Q., Chin, A., Wong, C.H., Wang, H., McFerrin, L., Selamat, S.A., Yang, C., Kroh, E.M., Garg, K.S., Behrens, C., Gazdar, A.F., Laird-Offringa, I.A., Tewari, M., Wistuba, I.I., Thiery, J.P., Hanash, S.M., 2015. Molecular portraits of epithelial, mesenchymal, and hybrid States in lung adenocarcinoma and their relevance to survival. Cancer Res. 75, 1789–1800.
Schoppmann, S.F., Schindl, M., Bayer, G., Aumayr, K., Dienes, J., Horvat, R., Rudas, M., Gnant, M., Jakesz, R., Birner, P., 2003. Overexpression of Id-1 is associated with poor clinical outcome in node negative breast cancer. Int. J. Cancer 104, 677–682.
Sciacca, M.F.M., Romanucci, V., Zarrelli, A., Monaco, I., Lolicato, F., Spinella, N., Galati, C., Grasso, G., D'Urso, L., Romeo, M., Diomede, L., Salmona, M., Bongiorno, C., Di Fabio, G., La Rosa, C., Milardi, D., 2017. Inhibition of Aβ amyloid growth and toxicity by silybins: the crucial role of stereochemistry. ACS Chem. Neurosci. 8, 1767–1778.
Sharma, P., Patel, D., Chaudhary, J., 2012. Id1 and Id3 expression is associated with increasing grade of prostate cancer: id3 preferentially regulates CDKN1B. Cancer Med. 1, 187–197.
Shepherd, T.G., Thériault, B.L., Nachtigal, M.W., 2008. Autocrine BMP4 signalling regulates ID3 proto-oncogene expression in human ovarian cancer cells. Gene 414, 95–105.
Solar, P., Hendrych, M., Barak, M., Valekova, H., Hermanova, M., Jancalek, R., 2022. Blood-brain barrier alterations and edema formation in different brain mass lesions. Front. Cell. Neurosci. 16, 922181.
Stankic, M., Pavlovic, S., Chin, Y., Brogi, E., Padua, D., Norton, L., Massagué, J., Benezra, R., 2013. TGF-β-Id1 signaling opposes Twist1 and promotes metastatic colonization via a mesenchymal-to-epithelial transition. Cell Rep. 5, 1228–1242.
Teo, W.S., Holliday, H., Karthikeyan, N., Cazet, A.S., Roden, D.L., Harvey, K., Konrad, C. V., Murali, R., Varghese, B.A., Thankamony, A.P., Chan, C.L., McFarland, A., Junankar, S., Ye, S., Yang, J., Nikolic, I., Shah, J.S., Baker, L.A., Millar, E.K.A., Naylor, M.J., Ormandy, C.J., Lakhani, S.R., Kaplan, W., Mellick, A.S., O'Toole, S.A., Swarbrick, A., Nair, R., 2020. Id proteins promote a cancer stem cell phenotype in mouse models of triple negative breast cancer via negative regulation of robo1. Front. Cell. Dev. Biol. 8, 552.
Thompson, J.C., Hwang, W.T., Davis, C., Deshpande, C., Jeffries, S., Rajpurohit, Y., Krishna, V., Smirnov, D., Verona, R., Lorenzi, M.V., Langer, C.J., Albelda, S.M., 2020. Gene signatures of tumor inflammation and epithelial-to-mesenchymal transition (EMT) predict responses to immune checkpoint blockade in lung cancer with high accuracy. Lung Cancer 139, 1–8.
Thomson, S., Buck, E., Petti, F., Griffin, G., Brown, E., Ramnarine, N., Iwata, K.K., Gibson, N., Haley, J.D., 2005. Epithelial to mesenchymal transition is a determinant of sensitivity of non-small-cell lung carcinoma cell lines and xenografts to epidermal growth factor receptor inhibition. Cancer Res. 65, 9455–9462.
Varma, D.A., Tiwari, M., 2021. Crizotinib-induced anti-cancer activity in human cervical carcinoma cells via ROS-dependent mitochondrial depolarization and induction of apoptotic pathway. J. Obstet. Gynaecol. Res. 47, 3923–3930.
Vazquez-Martin, A., Cufí, S., Oliveras-Ferraros, C., Torres-Garcia, V.Z., Corominas-Faja, B., Cuyàs, E., Bonavia, R., Visa, J., Martin-Castillo, B., Barrajón-Catalán, E., Micol, V., Bosch-Barrera, J., Menendez, J.A., 2013. IGF-1R/epithelial-to-mesenchymal transition (EMT) crosstalk suppresses the erlotinib-sensitizing effect of EGFR exon 19 deletion mutations. Sci. Rep. 3, 2560.
Verdura, S., Cuyàs, E., Llorach-Parés, L., Pérez-Sánchez, A., Micol, V., Nonell-Canals, A., Joven, J., Valiente, M., Sánchez-Martínez, M., Bosch-Barrera, J., Menendez, J.A., 2018. Silibinin is a direct inhibitor of STAT3. Food Chem. Toxicol. 116, 161–172.
Verdura, S., Cuyàs, E., Ruiz-Torres, V., Micol, V., Joven, J., Bosch-Barrera, J., Menendez, J.A., 2021. Lung cancer management with silibinin: a historical and translational perspective. Pharmaceuticals (Basel) 14, 559.
Verdura, S., Encinar, J.A., Teixidor, E., Segura-Carretero, A., Micol, V., Cuyàs, E., Bosch-Barrera, J., Menendez, J.A., 2022. Silibinin overcomes EMT-driven lung cancer resistance to new-generation ALK inhibitors. Cancers (Basel) 14, 6101.
Wang, C., Wang, Z., Zhang, X., Zhang, X., Dong, L., Xing, Y., Li, Y., Liu, Z., Chen, L., Qiao, H., Wang, L., Zhu, C., 2012. Protection by silibinin against experimental ischemic stroke: up-regulated pAkt, pmTOR, HIF-1α and Bcl-2, down-regulated Bax, NF-κB expression. Neurosci. Lett. 529, 45–50.
Wang, L.H., Baker, N.E., 2015. E proteins and ID proteins: helix-loop-helix partners in development and disease. Dev. Cell. 35, 269–280.
Wasilewski, D., Priego, N., Fustero-Torre, C., Valiente, M., 2017. Reactive astrocytes in brain metastasis. Front. Oncol. 7, 298.
Weksler, B.B., Subileau, E.A., Perrière, N., Charneau, P., Holloway, K., Leveque, M., Tricoire-Leignel, H., Nicotra, A., Bourdoulous, S., Turowski, P., Male, D.K., Roux, F., Greenwood, J., Romero, I.A., Couraud, P.O., 2005. Blood-brain barrier-specific properties of a human adult brain endothelial cell line. FASEB J. 19, 1872–1874.
Wojnarowicz, P.M., Escolano, M.G., Huang, Y.H., Desai, B., Chin, Y., Shah, R., Xu, S., Yadav, S., Yaklichkin, S., Ouerfelli, O., Soni, R.K., Philip, J., Montrose, D.C., Healey, J.H., Rajasekhar, V.K., Garland, W.A., Ratiu, J., Zhuang, Y., Norton, L., Rosen, N., Hendrickson, R.C., Zhou, X.K., Iavarone, A., Massague, J., Dannenberg, A. J., Lasorella, A., Benezra, R., 2021. Anti-tumor effects of an ID antagonist with no observed acquired resistance. NPJ Breast Cancer 7, 58.
Wojnarowicz, P.M., Lima E Silva, R., Ohnaka, M., Lee, S.B., Chin, Y., Kulukian, A., Chang, S.H., Desai, B., Garcia Escolano, M., Shah, R., Garcia-Cao, M., Xu, S., Kadam, R., Goldgur, Y., Miller, M.A., Ouerfelli, O., Yang, G., Arakawa, T., Albanese, S.K., Garland, W.A., Stoller, G., Chaudhary, J., Norton, L., Soni, R.K., Philip, J., Hendrickson, R.C., Iavarone, A., Dannenberg, A.J., Chodera, J.D., Pavletich, N., Lasorella, A., Campochiaro, P.A., Benezra, R., 2019. A small-molecule pan-id antagonist inhibits pathologic ocular neovascularization. Cell Rep. 29, 62–75.
Yamaguchi, N., Lucena-Araujo, A.R., Nakayama, S., de Figueiredo-Pontes, L.L., Gonzalez, D.A., Yasuda, H., Kobayashi, S., Costa, D.B., 2014. Dual ALK and EGFR inhibition targets a mechanism of acquired resistance to the tyrosine kinase inhibitor crizotinib in ALK rearranged lung cancer. Lung Cancer 83, 37–43.
Yan, H., Du, J., Chen, X., Yang, B., He, Q., Yang, X., Luo, P., 2019. ROS-dependent DNA damage contributes to crizotinib-induced hepatotoxicity via the apoptotic pathway. Toxicol. Appl. Pharmacol. 383, 114768.
Yang, J., Li, X., Morrell, N.W., 2014. Id proteins in the vasculature: from molecular biology to cardiopulmonary medicine. Cardiovasc. Res. 104, 388–398.
Ying, Q.L., Nichols, J., Chambers, I., Smith, A., 2003. BMP induction of Id proteins suppresses differentiation and sustains embryonic stem cell self-renewal in collaboration with STAT3. Cell 115, 281–292.